Compressed Sensing in Optics: Schlieren Deflectometry and Refractive Index Map Reconstruction

Joint work with:

P. Sudhakar*, A. Gonzalez*, C. De Vleeschouwer*,

X. Dubois[+], P. Antoine[+], Luc Joannes[+]

 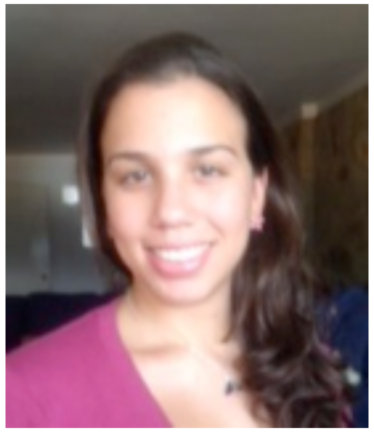    

*: Louvain University (UCL), Louvain-la-Neuve, Belgium

[+]: Lambda-X, Nivelles, Belgium

Compressive Sampling

Compressed Sensing

Part I:

Highly compressed recap of what is ...

Compressive Sensing

Compressed Sampling

Generally, sampling is ...

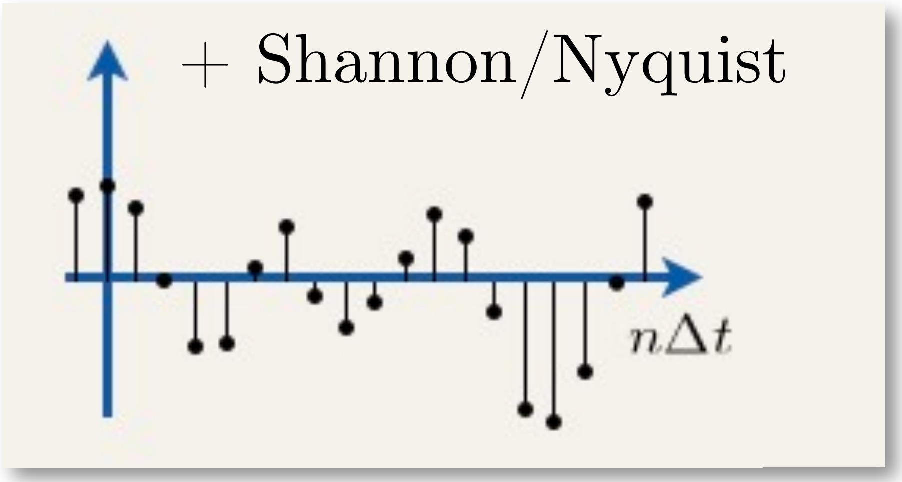

Human readable signal!

Generally, sampling is ...

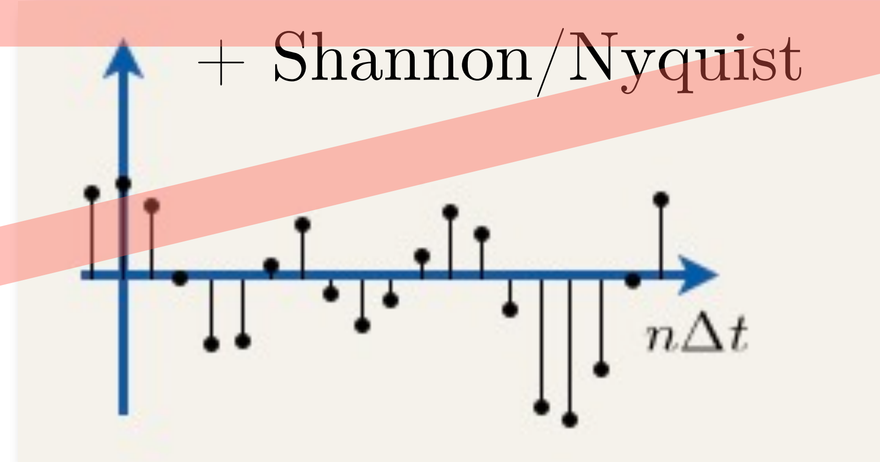

Human readable signal

New ways to sample signals ....

"*Computer readable*" sensing + prior information

World → Signal → Sensing Device → Sensing →

→ Signal → Human

Optimized setup: sampling rate $\propto$ information

Generally, sampling is ...

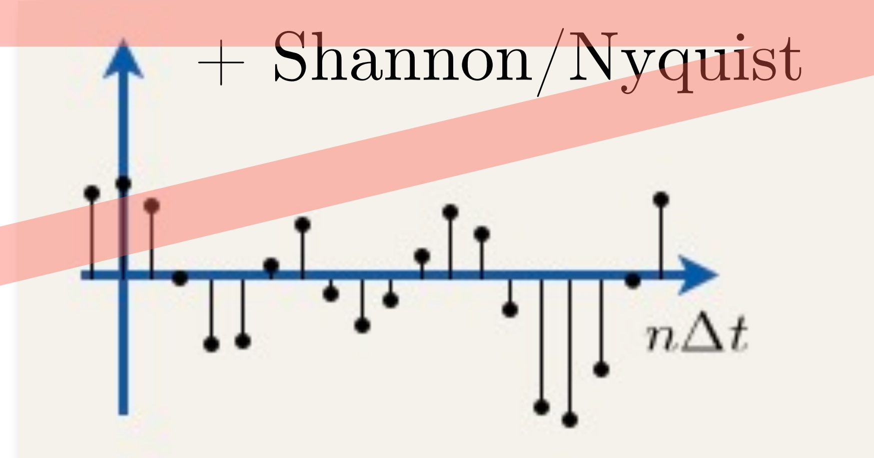

Human readable signal

New ways to sample signals ....

structures, sparsity, low-rank, ...

"*Computer readable*" sensing + prior information

World → Signal → Sensing Device → Sensing →  → Signal → Human

Optimized setup: sampling rate $\propto$ information

Compressed Sensing...

... in a nutshell:

> "Forget" Dirac, forget Nyquist,
> ask *few* (**linear**) *questions*
> about your informative (**sparse**) signal,
> and recover it *differently* (**non-linearly**)"

1st, CS $\ni$ Generalized Linear Sensing!

M questions — Sensing method — Signal

$\boldsymbol{y}$ $\quad$ $\boldsymbol{\Phi}$ $\quad$ $\boldsymbol{x}$

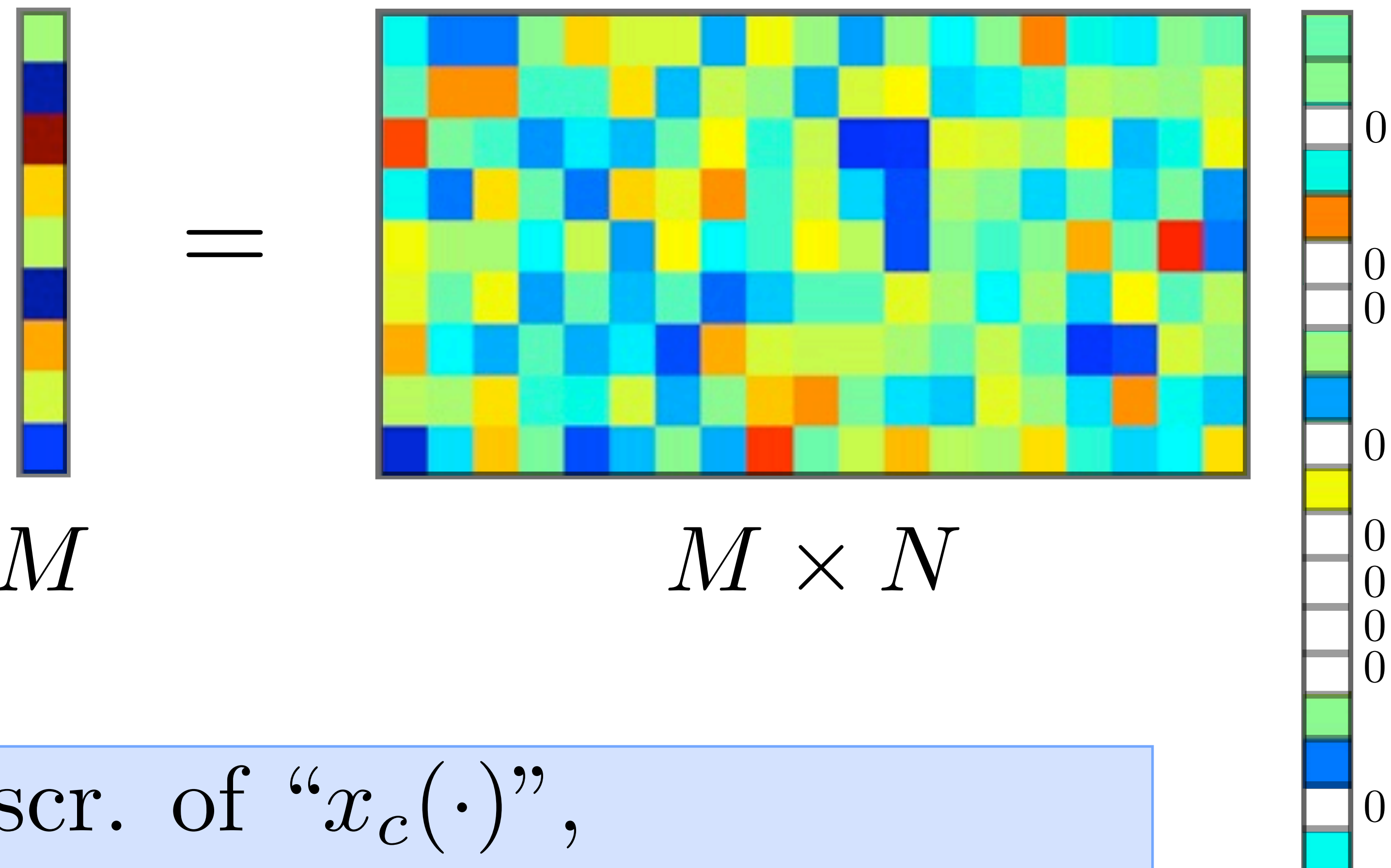

M $\qquad$ $M \times N$ $\qquad$ N

Sparsity Prior ($\Psi = \mathrm{Id}$)

A signal in this discrete world

Caveat: $\boldsymbol{x}$ = discr. of "$x_c(\cdot)$",
and $\boldsymbol{y} = \Phi(x_c) \approx \boldsymbol{\Phi x}$
given some (linear) sensing Φ process of x_c

1st, CS $\ni$ Generalized Linear Sensing!

M questions — Sensing method — Signal

$\boldsymbol{y}$ $\quad \boldsymbol{\Phi} \quad$ $\boldsymbol{x}$

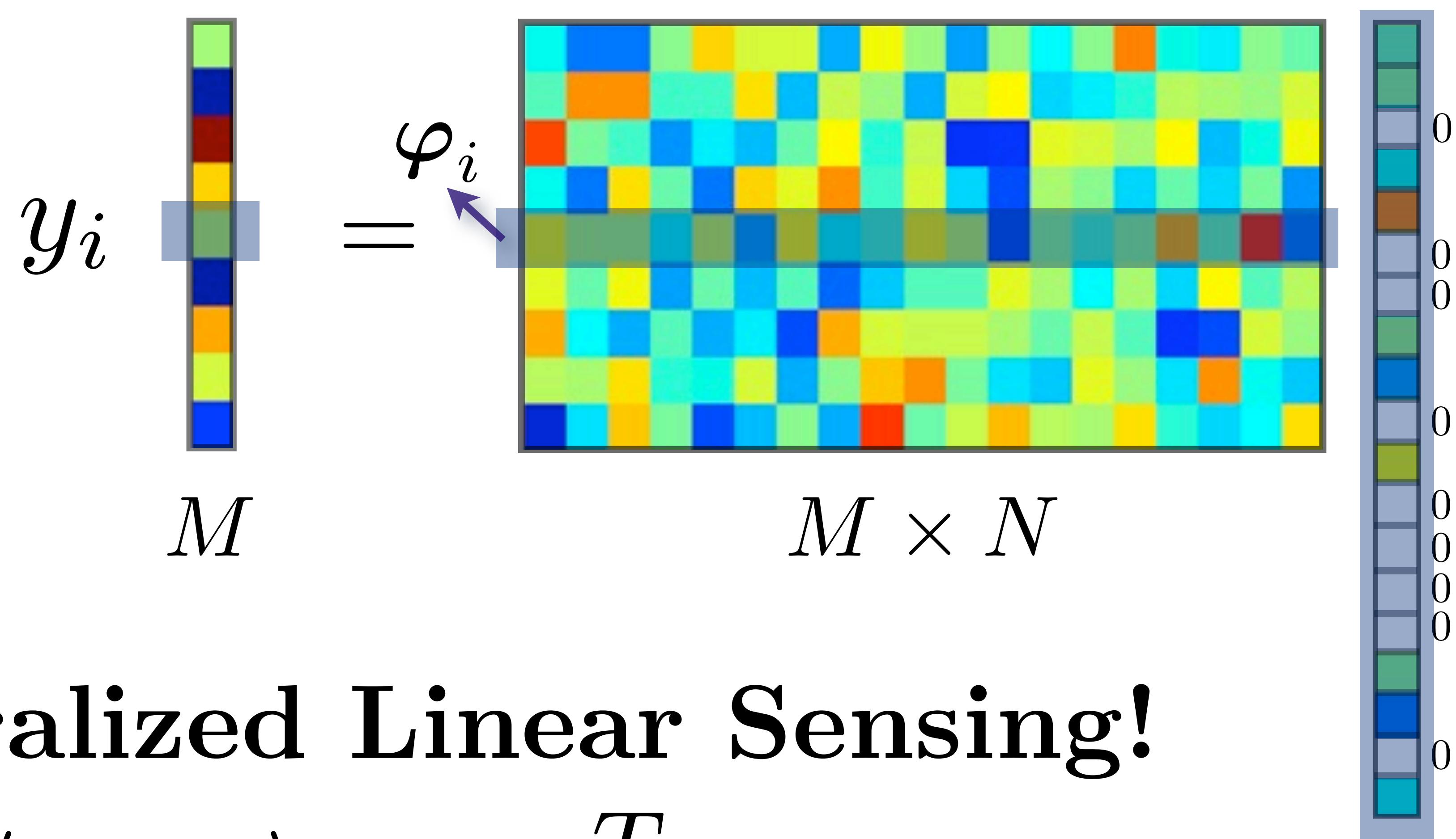

M $\quad$ $M \times N$ $\quad$ N

Sparsity Prior ($\Psi = \mathrm{Id}$)

A signal in this discrete world

Generalized Linear Sensing!

$$y_i = \langle \boldsymbol{\varphi}, \boldsymbol{x} \rangle = \boldsymbol{\varphi}^T \boldsymbol{x}$$

$$1 \leq i \leq M$$

e.g., to be realized optically!

2nd, CS $\ni$ Non-linear reconstruction!

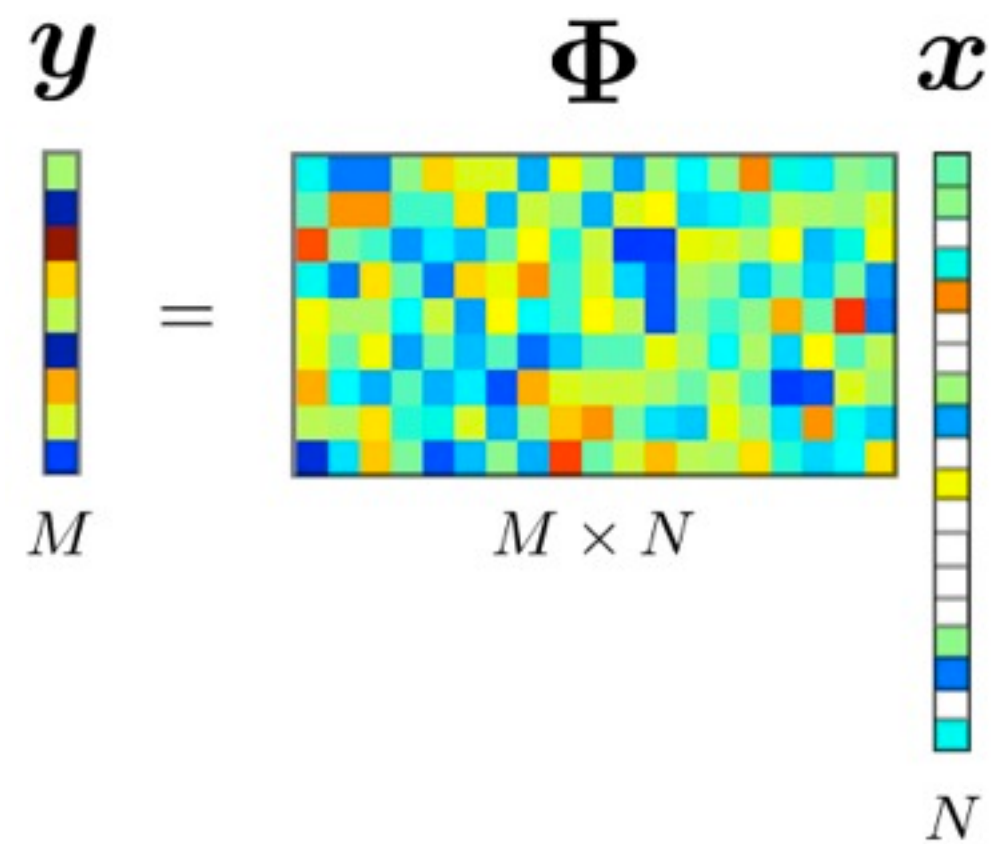

If $\boldsymbol{x}$ is K-sparse and if $\boldsymbol{\Phi}$ well "conditioned"
then:

$$\boldsymbol{x}^* = \underset{\boldsymbol{u} \in \mathbb{R}^N}{\arg\min} \; \|\boldsymbol{u}\|_1 \text{ s.t. } \boldsymbol{y} = \boldsymbol{\Phi}\boldsymbol{u}$$

$\|\boldsymbol{u}\|_1 = \sum_j |u_j|$ (Basis Pursuit) [Chen, Donoho, Saunders, 1998]

2nd, CS $\ni$ Non-linear reconstruction!

Simplifying assumption

$\exists\ \delta \in (0,1)$ Restricted Isometry Property

$$\sqrt{1-\delta}\,\|\boldsymbol{v}\|_2 \ \leqslant\ \|\boldsymbol{\Phi v}\|_2 \ \leqslant\ \sqrt{1+\delta}\,\|\boldsymbol{v}\|_2$$

for all $2K$ sparse signals $\boldsymbol{v}$.

any subset of $2K$ columns
is an *isometry*

If $\boldsymbol{x}$ is K-sparse and if $\boldsymbol{\Phi}$ well "conditioned"
then:

$$\boldsymbol{x}^* \ =\ \arg\min_{\boldsymbol{u}\in\mathbb{R}^N}\ \|\boldsymbol{u}\|_1 \text{ s.t. } \boldsymbol{y} = \boldsymbol{\Phi u}$$

if $\delta < \sqrt{2}-1$ [Candes 08]

$\|\boldsymbol{u}\|_1 = \sum_j |u_j|$

(Basis Pursuit) [Chen, Donoho, Saunders, 1998]

2nd, CS $\ni$ Non-linear reconstruction!

Simplifying assumption

$\exists\, \delta \in (0,1)$ Restricted Isometry Property

$$\sqrt{1-\delta}\,\|\boldsymbol{v}\|_2 \;\leqslant\; \|\boldsymbol{\Phi v}\|_2 \;\leqslant\; \sqrt{1+\delta}\,\|\boldsymbol{v}\|_2$$

for all $2K$ sparse signals $\boldsymbol{v}$.

any subset of $2K$ columns

is an *isometry*

Examples:

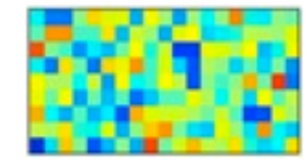

+ Gaussian
+ Bernoulli
+ Random Fourier
+ ....

$$M = O(K \log N/K) \ll N$$

$$\boldsymbol{\Phi} \in \mathbb{R}^{M\times N},\quad \Phi_{ij} \sim_{\text{iid}} \mathcal{N}(0,1)$$

If $\boldsymbol{x}$ is K-sparse and if $\boldsymbol{\Phi}$ well "conditioned"

then:

$$\boldsymbol{x}^* \;=\; \underset{\boldsymbol{u}\in\mathbb{R}^N}{\arg\min}\; \|\boldsymbol{u}\|_1 \text{ s.t. } \boldsymbol{y} = \boldsymbol{\Phi u}$$

if $\delta < \sqrt{2} - 1$ [Candes 08]

$\|\boldsymbol{u}\|_1 = \sum_j |u_j|$ (Basis Pursuit) [Chen, Donoho, Saunders, 1998]

2nd, CS $\ni$ Non-linear reconstruction!

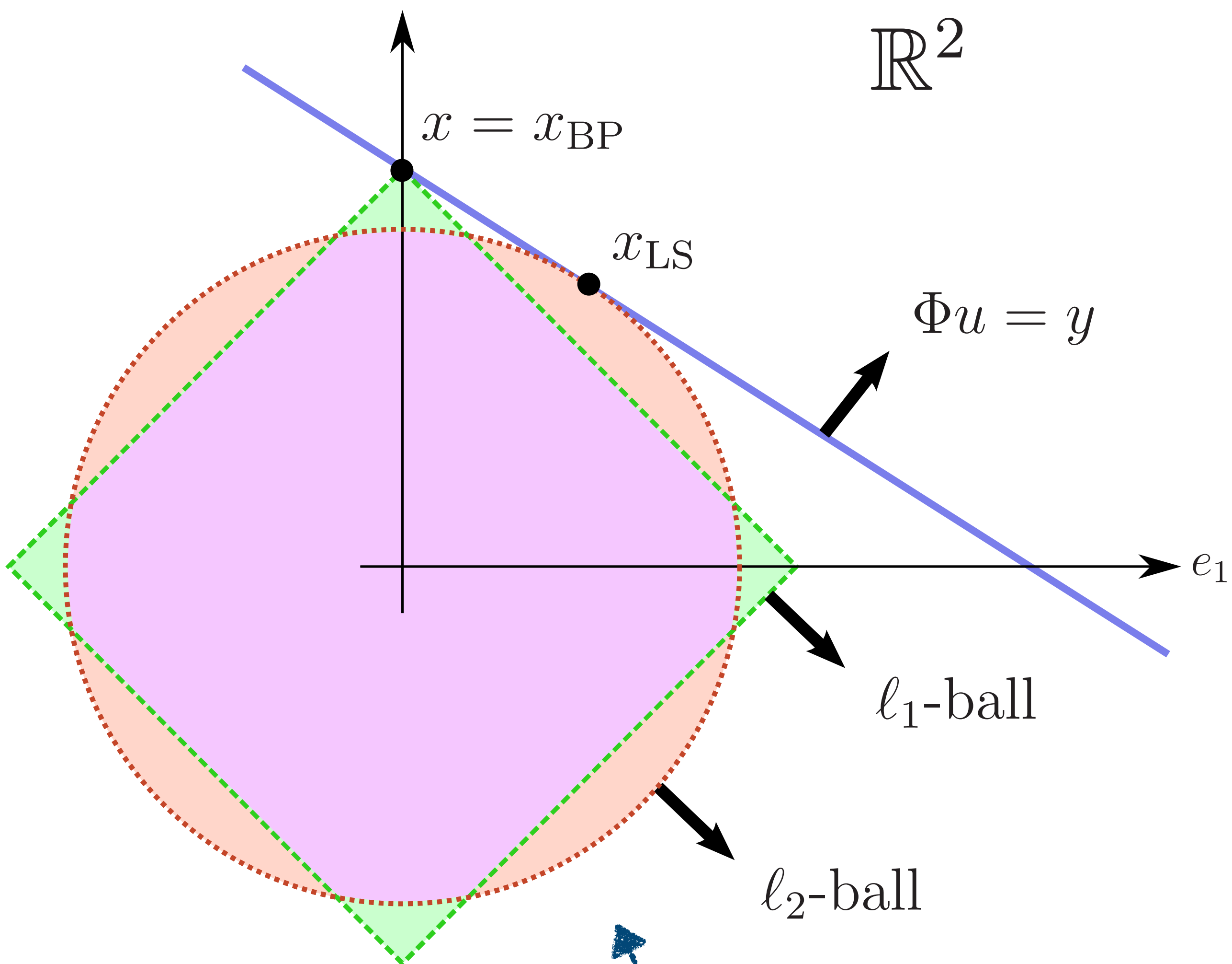

If $\boldsymbol{x}$ is K-sparse and if $\boldsymbol{\Phi}$ well "conditioned" then:

$$\boldsymbol{x}^* \;=\; \underset{\boldsymbol{u}\in\mathbb{R}^N}{\arg\min}\ \|\boldsymbol{u}\|_1 \text{ s.t. } \boldsymbol{y} = \boldsymbol{\Phi}\boldsymbol{u}$$

Solvers:

Linear Programming,
Interior Point Method,
Proximal Methods,
... **Tons** of toolboxes ...

$\|\boldsymbol{u}\|_1 = \sum_j |u_j|$

(Basis Pursuit) [Chen, Donoho, Saunders, 1998]

2nd, CS $\ni$ Non-linear reconstruction!

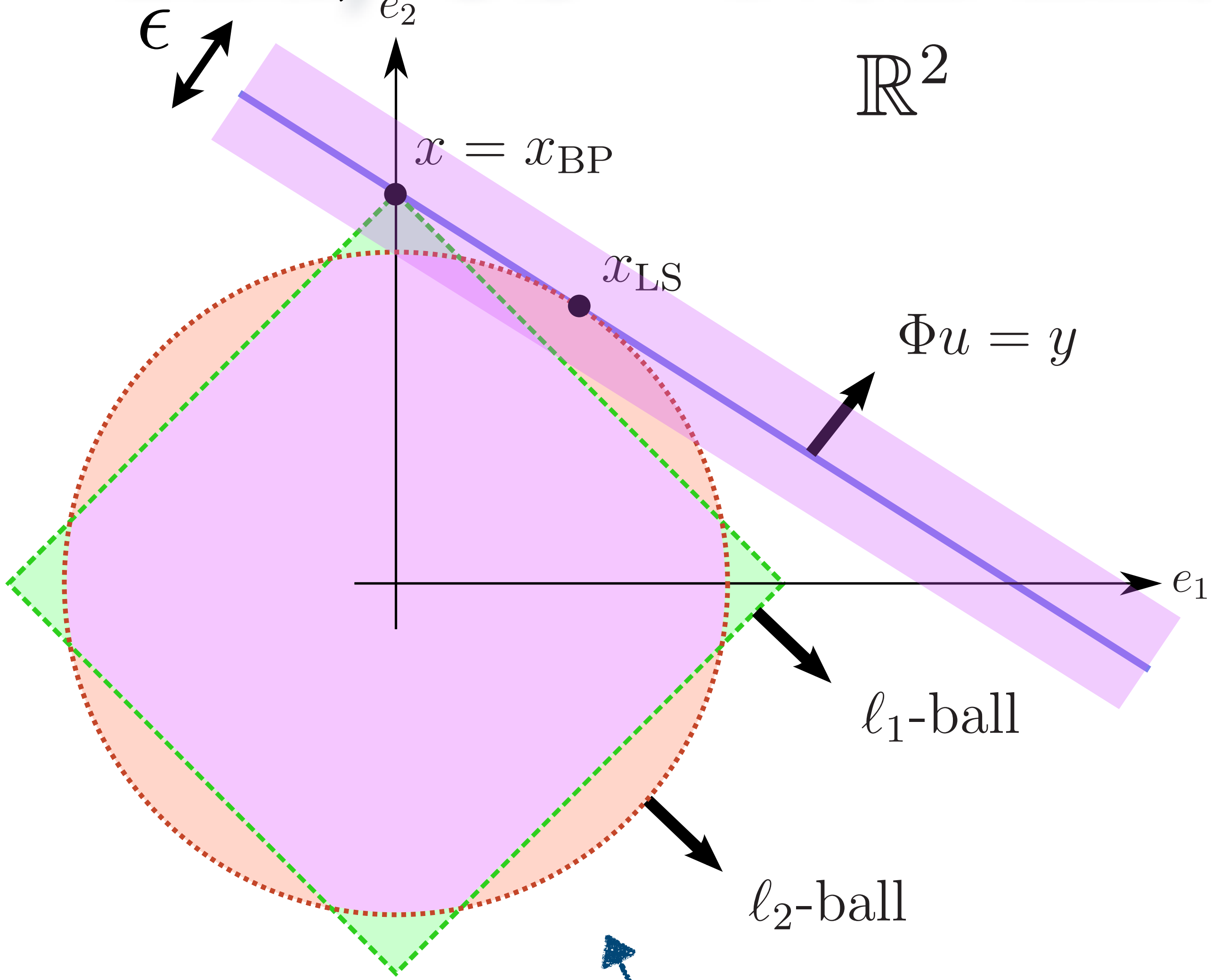

If $\boldsymbol{x}$ is K-sparse and if $\boldsymbol{\Phi}$ well "conditioned"
then:

$$\|\boldsymbol{y} - \boldsymbol{\Phi u}\| \leqslant \epsilon$$

$$\boldsymbol{x}^* = \underset{\boldsymbol{u} \in \mathbb{R}^N}{\arg\min} \ \|\boldsymbol{u}\|_1 \ \text{s.t.}\ \boldsymbol{y} = \boldsymbol{\Phi u}$$

$\|\boldsymbol{u}\|_1 = \sum_j |u_j|$

(Basis Pursuit) [Chen, Donoho, Saunders, 1998]

Solvers:

Linear Programming,
Interior Point Method,
Proximal Methods,
... **Tons** of toolboxes ...

2nd, CS $\ni$ Non-linear reconstruction!

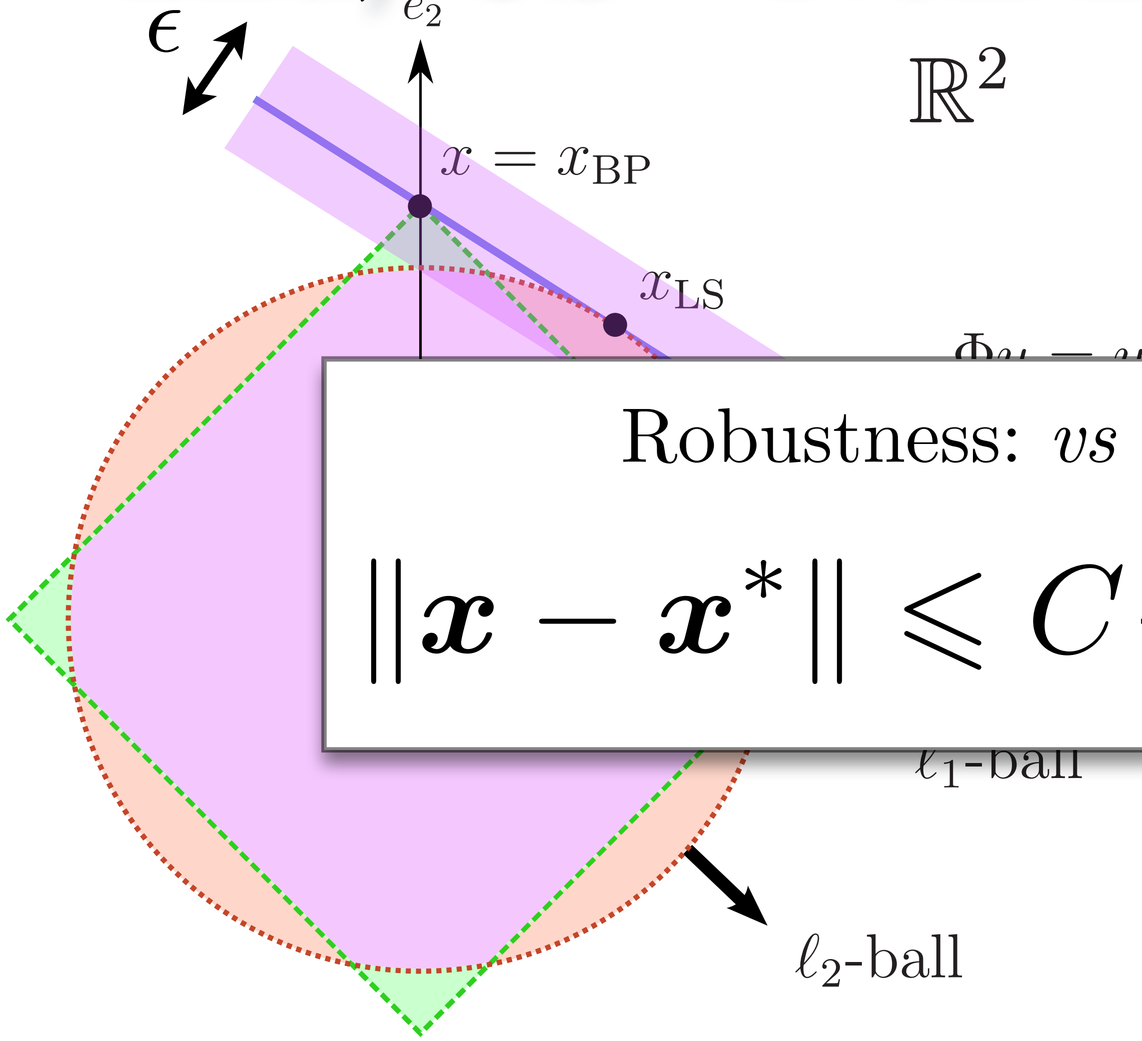

Robustness: *vs* sparse deviation + noise.

$$\|\boldsymbol{x} - \boldsymbol{x}^*\| \leqslant C \frac{1}{\sqrt{K}} \|\boldsymbol{x} - \boldsymbol{x}_K\|_1 + D\epsilon$$

If $\boldsymbol{x}$ is K-sparse and if $\boldsymbol{\Phi}$ well "conditioned" then:

$$\|\boldsymbol{y} - \boldsymbol{\Phi u}\| \leqslant \epsilon$$

(relax.)

$$\boldsymbol{x}^* \;=\; \mathop{\arg\min}_{\boldsymbol{u} \in \mathbb{R}^N} \|\boldsymbol{u}\|_1 \text{ s.t. } \boldsymbol{y} = \boldsymbol{\Phi u}$$

$\|\boldsymbol{u}\|_1 = \sum_j |u_j|$

(Basis Pursuit) [Chen, Donoho, Saunders, 1998]

Solvers:

Linear Programming,
Interior Point Method,
Proximal Methods,
... **Tons** of toolboxes ...

Part II:
Compressive Schlieren Deflectometry

(main contributor: Prasad Sudhakar
+ Lambda-X collaboration)

The problem:

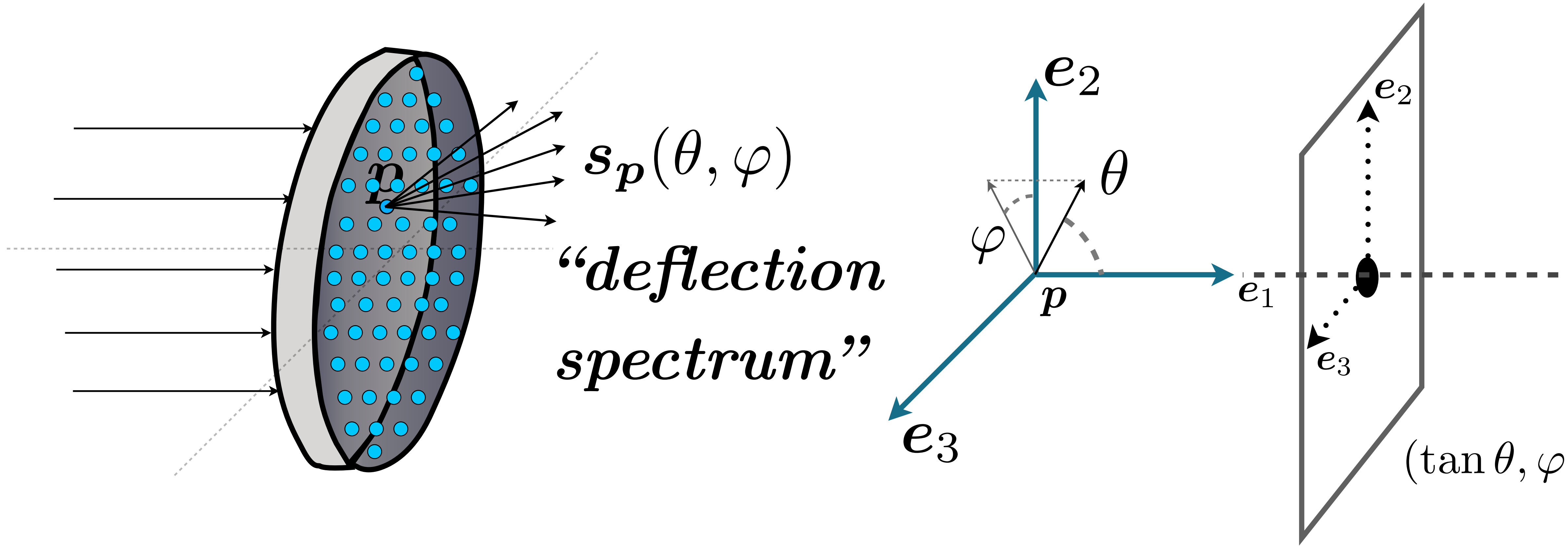

- Local curvature at every $\boldsymbol{p}$ is characterized by $\boldsymbol{s_p}(\theta, \varphi)$
- Objective: Reconstruct deflection spectra at all $\boldsymbol{p}$
- Application: Optical manufacturing and metrology

Deflection spectrum:

- Observation:

  Smooth objects = controlled deflections = ***sparse*** deflection spectra

- Difficult to measure deflections directly

  Only indirect measurement

- Tool: Schlieren Deflectometry

  Light changes its path based on refractive index change

- Noisy problem!

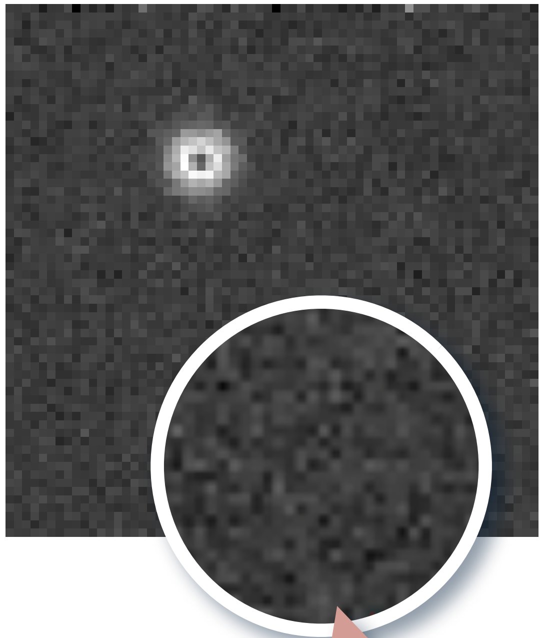

Schlieren deflectometry:

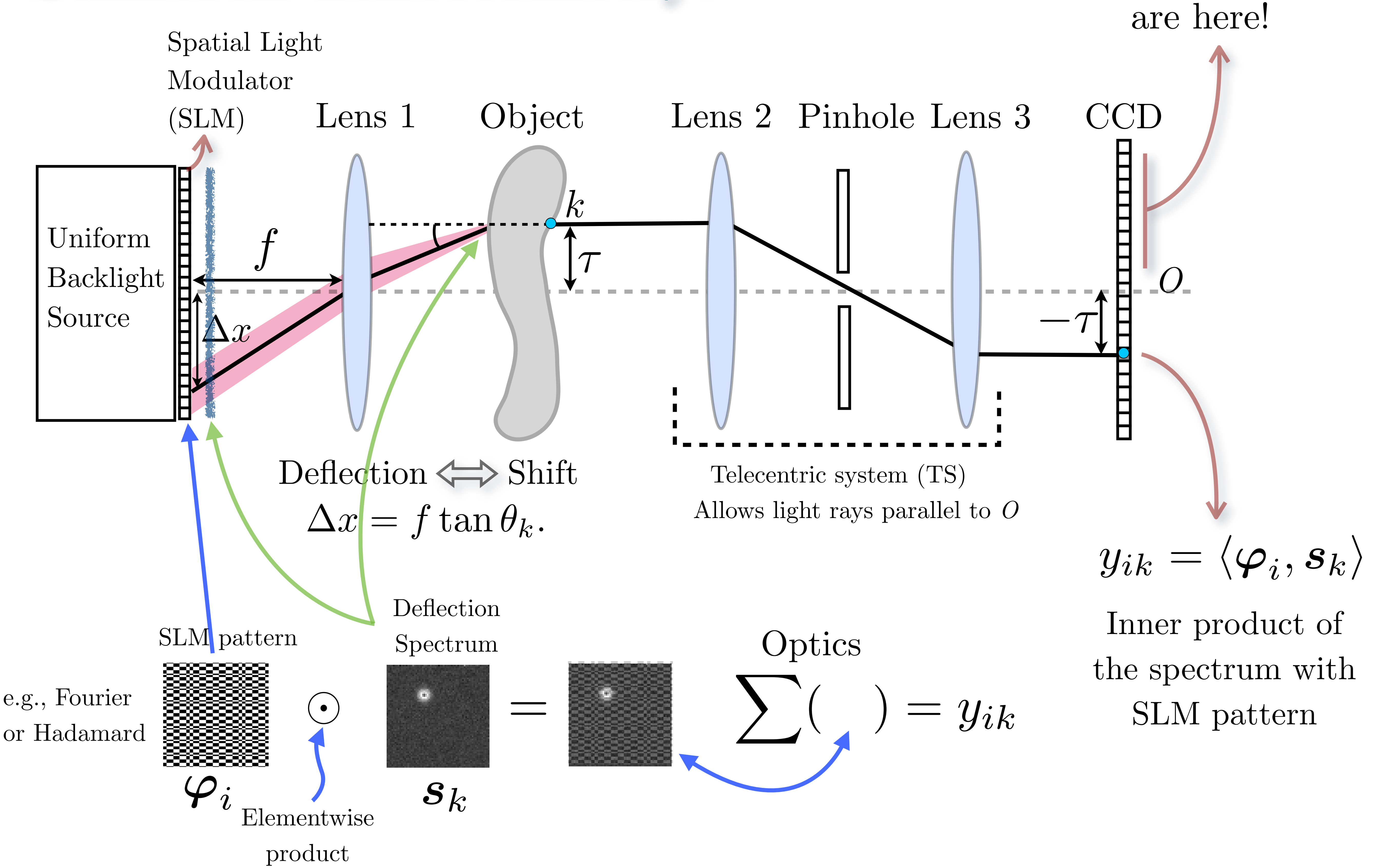

A system view ...

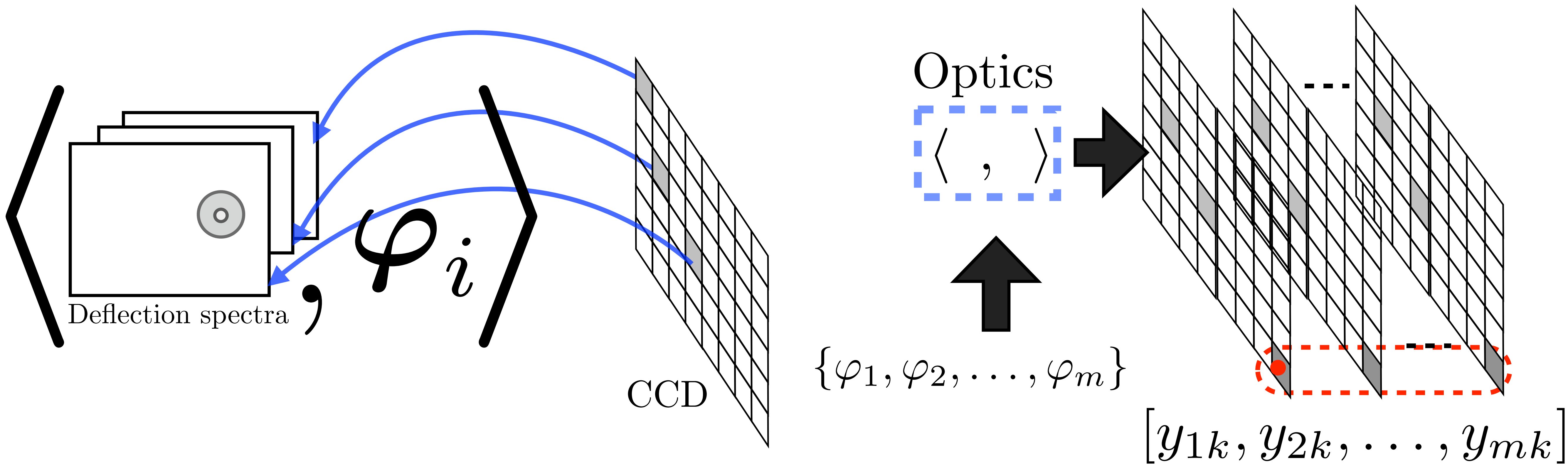

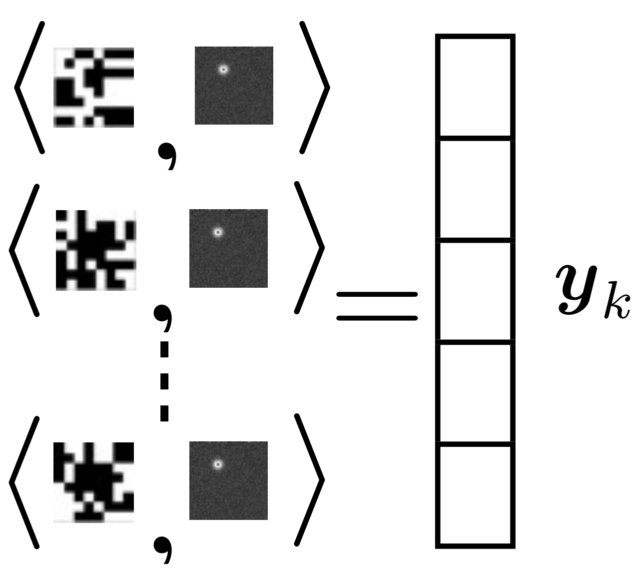

Vector of *measurements*

Deflection spectrum (as a vector)

$$\boldsymbol{y}_k = \boxed{\boldsymbol{\Phi}}\boldsymbol{s}_k + \boldsymbol{n}$$

Measurement noise

SLM patterns (as rows)

The inverse problem

$$\boldsymbol{y}_k = \boldsymbol{\Phi} \boldsymbol{s}_k + \boldsymbol{n}$$

- For each pixel k, Obtain $\boldsymbol{s}_k$ from $\boldsymbol{y}_k$

- Operational requirement
  - Fewer SLM patterns = small sized $\boldsymbol{y}_k$

  underdetermined linear inverse problem

- What helps?
  - sparse deflection spectra $\boldsymbol{s}_k$
  - pattern randomness

Compressive Sensing (CS)

CS of deflection spectra

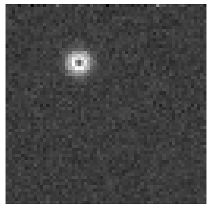

$\Longleftrightarrow \boldsymbol{s}_k$

Sparse Deflection spectrum

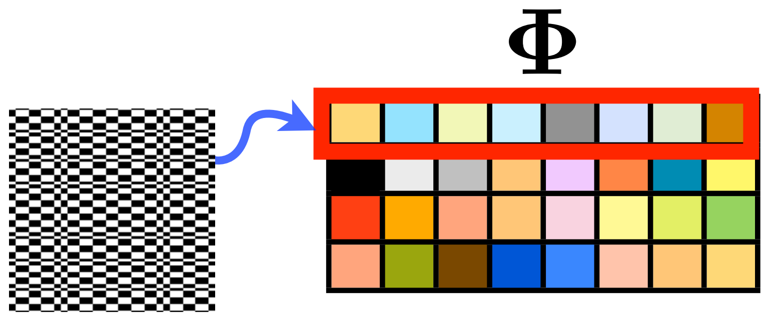

SLM patterns = Sensing matrix

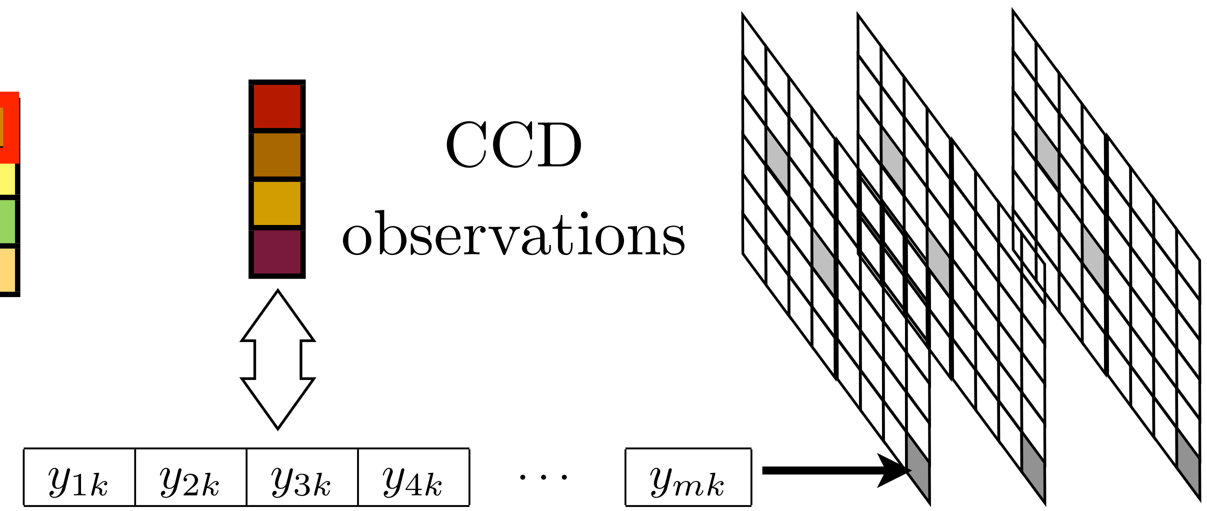

$$\boldsymbol{s}_k = \boldsymbol{\Psi}\boldsymbol{\alpha}_k \qquad \boldsymbol{y}_k = \boldsymbol{\Phi}\boldsymbol{s}_k = \boldsymbol{\Phi}\boldsymbol{\Psi}\boldsymbol{\alpha}_k$$

- Rice University's single pixel camera

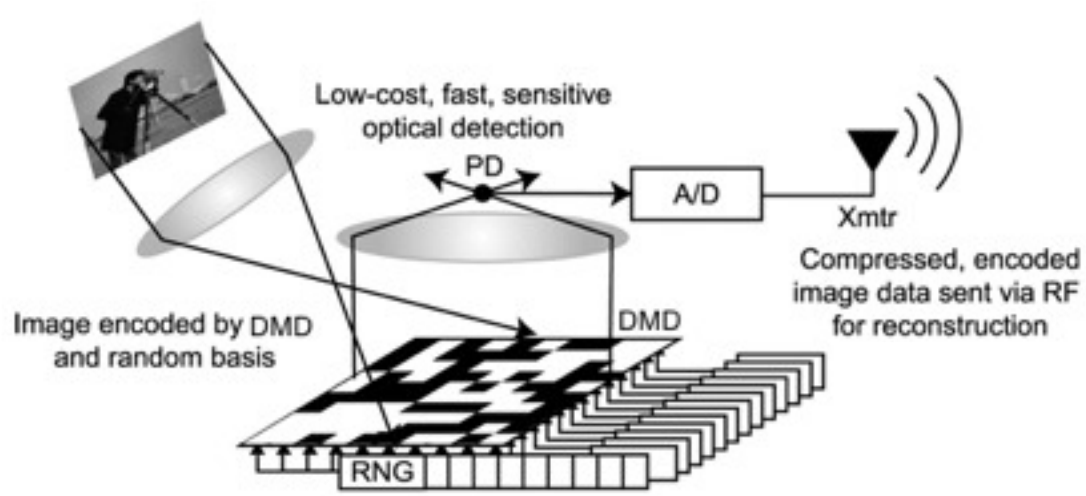

Image credits: Rice University
http://dsp.rice.edu/cscamera

Each CCD pixel of Schlieren deflectometer = single pixel camera

What are the sensing constraints ?

- Physical constraints of the system:
  - Non-negative, real-valued sensing matrix entries
  - Binary sensing matrix entries: avoiding non-linearities
- Additional requirements:
  - Randomness for optimal measurements
  - Structured measurements for fast computations

➠ **Spread Spectrum Compressive Sensing** [Puy et al, 2012]

Spread Spectrum Compressive Sensing 1/2

- $\boldsymbol{\Gamma} = \boldsymbol{H}$: Hadamard basis (binary)

  Need not be incoherent with the sparsity basis $\boldsymbol{\Psi}$

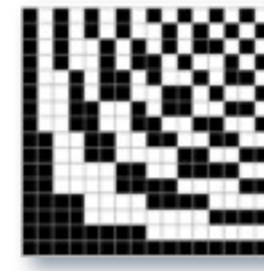

- Spread spectrum: random phase modulation of $\boldsymbol{s}$

  - Rademacher/ Steinhaus sequence

    $\boldsymbol{m}, \quad |m_i| = 1$

  - ***Spread spectrum matrix***

    $\boldsymbol{M} =$ 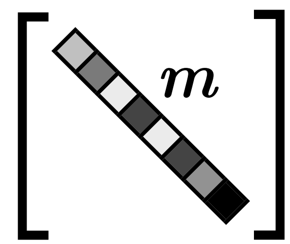

    $\in \mathbb{C}^{N \times N}$

  $$\boldsymbol{y} = \boldsymbol{H}_\Omega^T \boldsymbol{M} \boldsymbol{s}$$

  $$\boldsymbol{\Phi} = \boldsymbol{H}_\Omega^T \boldsymbol{M}$$

- Real valued $\boldsymbol{M} \Rightarrow m_i = \pm 1$ w.e.p. $\Rightarrow \boldsymbol{H}^T \boldsymbol{M} \in \{\pm 1\}^{N \times N}$

- Bias and scale for non-negativity: (since optical)

$$\boldsymbol{\Phi} = \frac{1}{2}(\boldsymbol{H}_\Omega^T \boldsymbol{M} + \mathbf{1}_N \mathbf{1}_N^T) \in \{0,1\}^{M \times N}$$

Spread Spectrum Compressive Sensing 2/2

- **Universal sensing bases** $|\Gamma_{ij}| = \text{ const.}$

  e.g., Fourier and Hadamard bases

- Successful recovery when $\boxed{M \geq C_\rho \, K \log^5(N)}$

  with a probability at least $1 - O(N^{-\rho})$, $0 < \rho < \log^3(N)$

  whatever the sparsity basis!!

  (principle: *coherence* decreasing with spread spec.)

G. Puy, et al., "Universal and efficient compressed sensing by spread spectrum and application to realistic Fourier imaging techniques," Journal on Adv. in Sig. Proc., 2012.

Reconstructions

Synthesis: $$\widehat{\boldsymbol{\alpha}} := \operatorname*{arg\,min}_{\boldsymbol{\alpha}\in\mathbb{C}^N} \|\boldsymbol{\alpha}\|_1 \text{ subject to } \|\boldsymbol{y} - \boldsymbol{\Phi}_{\mathrm{S}}\boldsymbol{\alpha}\|_2 \le \epsilon \text{ and } \boldsymbol{\Psi}\boldsymbol{\alpha} \in \mathbb{R}^N_+;$$

Reconstructions

Synthesis: $\widehat{\boldsymbol{\alpha}} := \arg\min_{\boldsymbol{\alpha}\in\mathbb{C}^N} \|\boldsymbol{\alpha}\|_1$ subject to $\|\boldsymbol{y} - \boldsymbol{\Phi}_{\mathrm{S}}\boldsymbol{\alpha}\|_2 \leq \epsilon$ and $\boldsymbol{\Psi}\boldsymbol{\alpha} \in \mathbb{R}^N_+$;

Analysis: ("beyond theory") $\hat{\boldsymbol{s}} := \arg\min_{\boldsymbol{s}} \|\boldsymbol{\Psi}^*\boldsymbol{s}\|_1$ subject to $\|\boldsymbol{y} - \boldsymbol{\Phi}_{\mathrm{A}}\boldsymbol{s}\|_2 \leq \epsilon$ and $\boldsymbol{s} \in \mathbb{R}^N_+$.

Reconstructions

Synthesis: $$\hat{\boldsymbol{\alpha}} := \arg\min_{\boldsymbol{\alpha}\in\mathbb{C}^N} \|\boldsymbol{\alpha}\|_1 \text{ subject to } \|\boldsymbol{y} - \boldsymbol{\Phi}_{\rm S}\boldsymbol{\alpha}\|_2 \le \epsilon \text{ and } \boldsymbol{\Psi}\boldsymbol{\alpha} \in \mathbb{R}^N_+;$$

Analysis: ("beyond theory") $$\hat{\mathrm{s}} := \arg\min_{\boldsymbol{s}} \|\boldsymbol{\Psi}^*\boldsymbol{s}\|_1 \text{ subject to } \|\boldsymbol{y} - \boldsymbol{\Phi}_{\rm A}\boldsymbol{s}\|_2 \le \epsilon \text{ and } \boldsymbol{s} \in \mathbb{R}^N_+.$$

- $\boldsymbol{\Psi}$: DWT & UDWT (Daubechies 9/7 wavelet basis)
- Additional constraint: Non-negative spectra
- Numerically: Proximal methods (Chambolle-Pock algorithm)
  - Generalized gradient methods for non-smooth convex functions
  - ***Proximal operators***: easy to evaluate for several functions
  - Easy to include additional constraints

(Not detailed here)

Noise estimation (an important part)

$\epsilon?$

- No test object: Physical model of deflection spectrum
  - deflection spectra = image of the pinhole.

a disk with a certain radius r and height h.

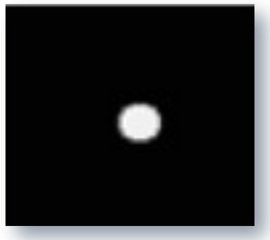

- Without any object, obtain $\boldsymbol{y}^{\rm no}$ with 100% measurements

$\boldsymbol{\Phi}^*\boldsymbol{y}^{\rm no}$

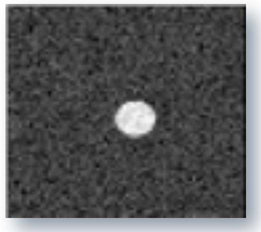

Reconstructed spectrum with $M = N$

-

$\boldsymbol{s}^{\rm no}$

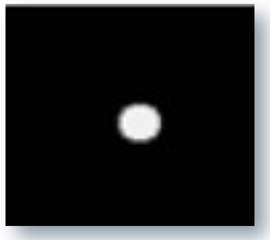

Model spectrum Numerically optimized r and h

=

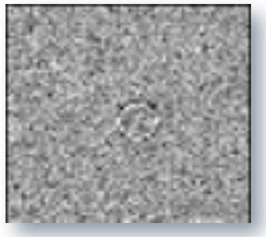

$\epsilon(N) = \Big\| \boldsymbol{y}^{\rm no} - \boldsymbol{\Phi}_{M=N}$ 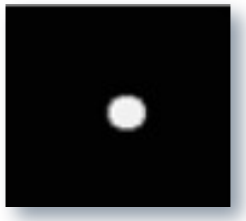 $\Big\|_2$

$$\boxed{\text{For } M < N, \quad \epsilon(M) = \sqrt{M + 2\sqrt{M}}\ \epsilon(N)/\sqrt{N}}$$

$\simeq 5\,\mathrm{dB}!$ (for all M)

Reconstruction results with experimental data

- Lambda-X NIMO system (9.99D plano-convex lens)
  - SLM size of 64×64 (one pixel "$\boldsymbol{k}$")

$\widehat{\boldsymbol{s}}_k$

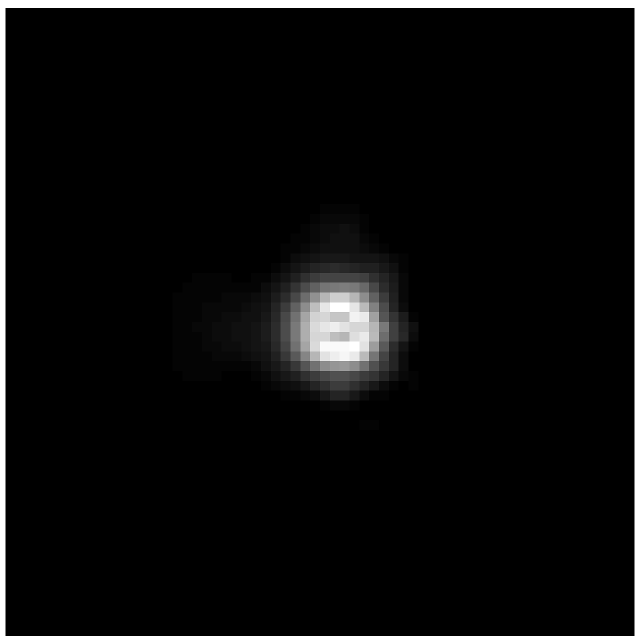

100% (M/N)

<u>Reminder</u>: input SNR $\simeq 5\,\mathrm{dB}$!

Reconstruction results with experimental data

- Lambda-X NIMO system (9.99D plano-convex lens)
  - SLM size of 64×64 (one pixel "$\boldsymbol{k}$")

$\widehat{\boldsymbol{s}}_k$

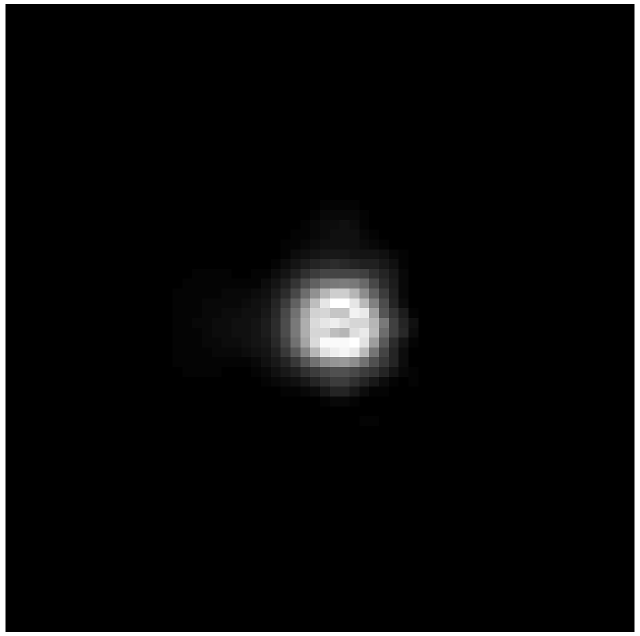

100% (M/N)

3.6% Synthesis DWT

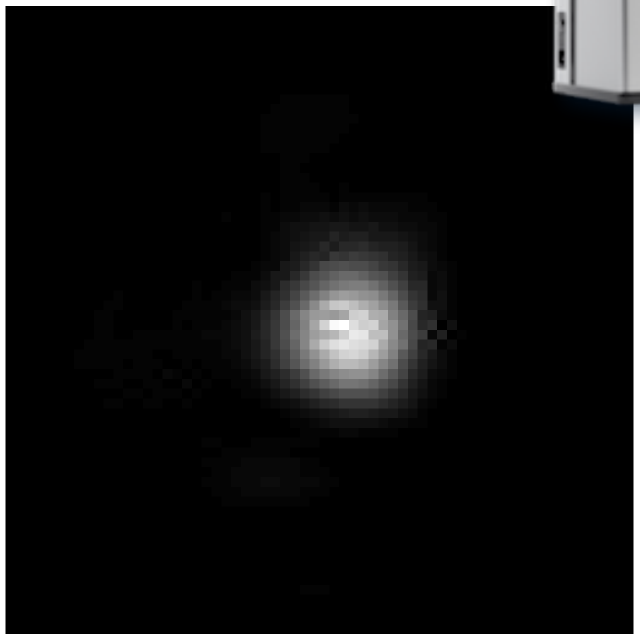

3.6% Analysis UDWT

(similar to synthesis UDWT)

<u>Reminder</u>: input SNR $\simeq 5\,\mathrm{dB}$!

Reconstruction results with experimental data

$\widehat{\boldsymbol{s}}_k$: Compressive sensing reconstruction

$\widehat{\boldsymbol{s}}_k^N$: spectrum reconstructed with 100% measurements.

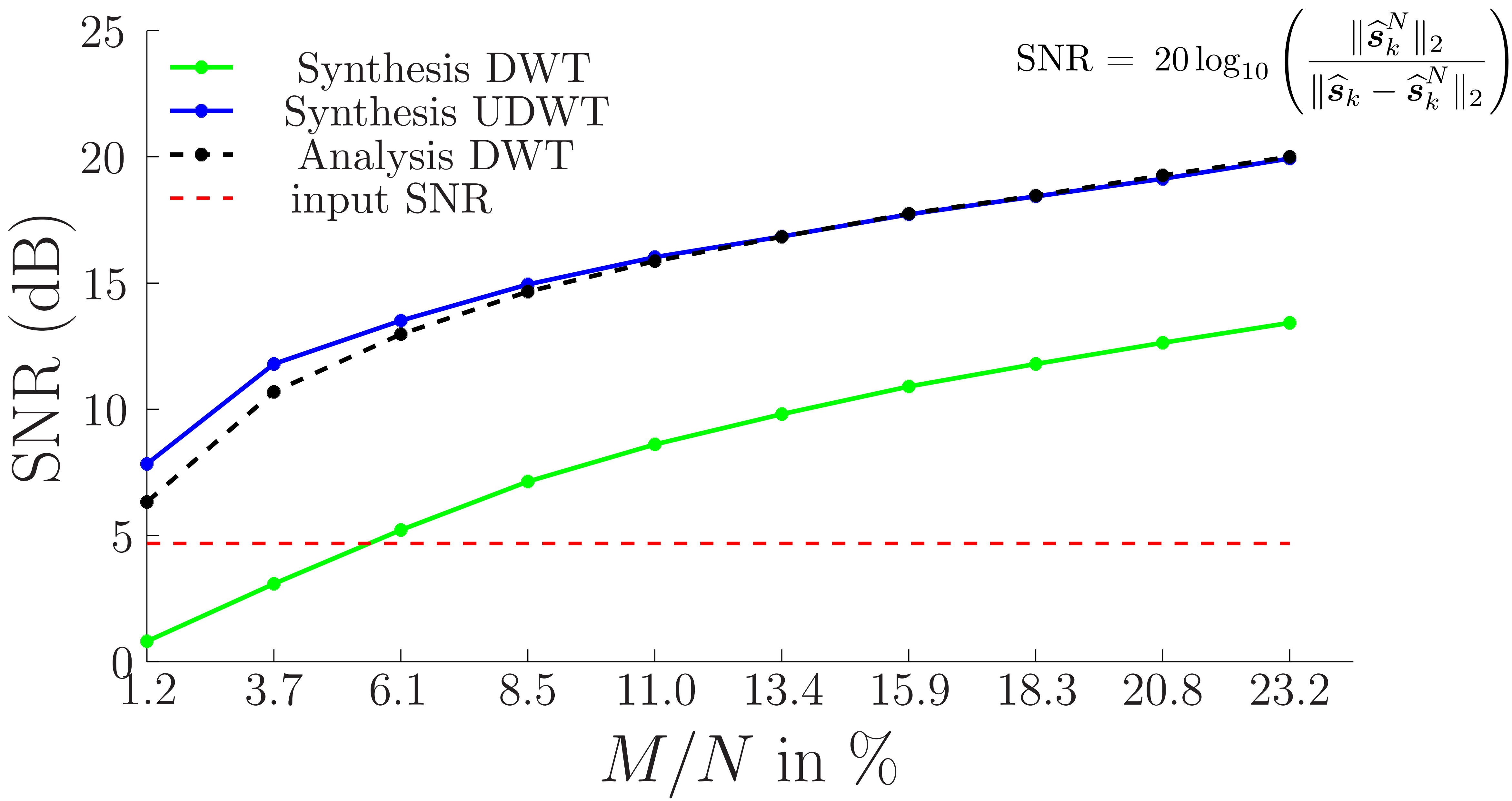

Deflection spectrum and the angles

Each object location $\Longleftrightarrow$ one deflection spectrum

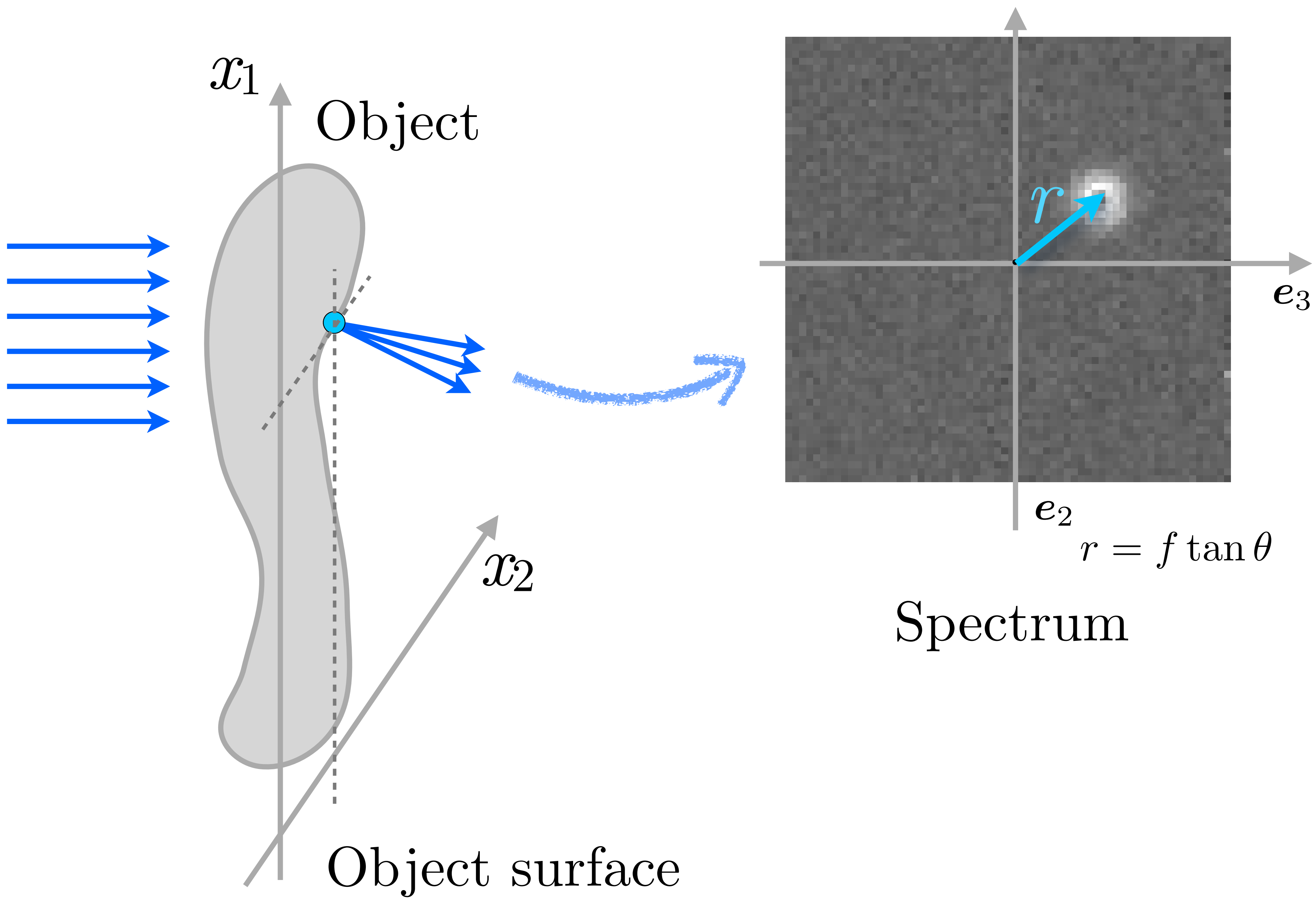

Deflection radius r vs CCD pixel

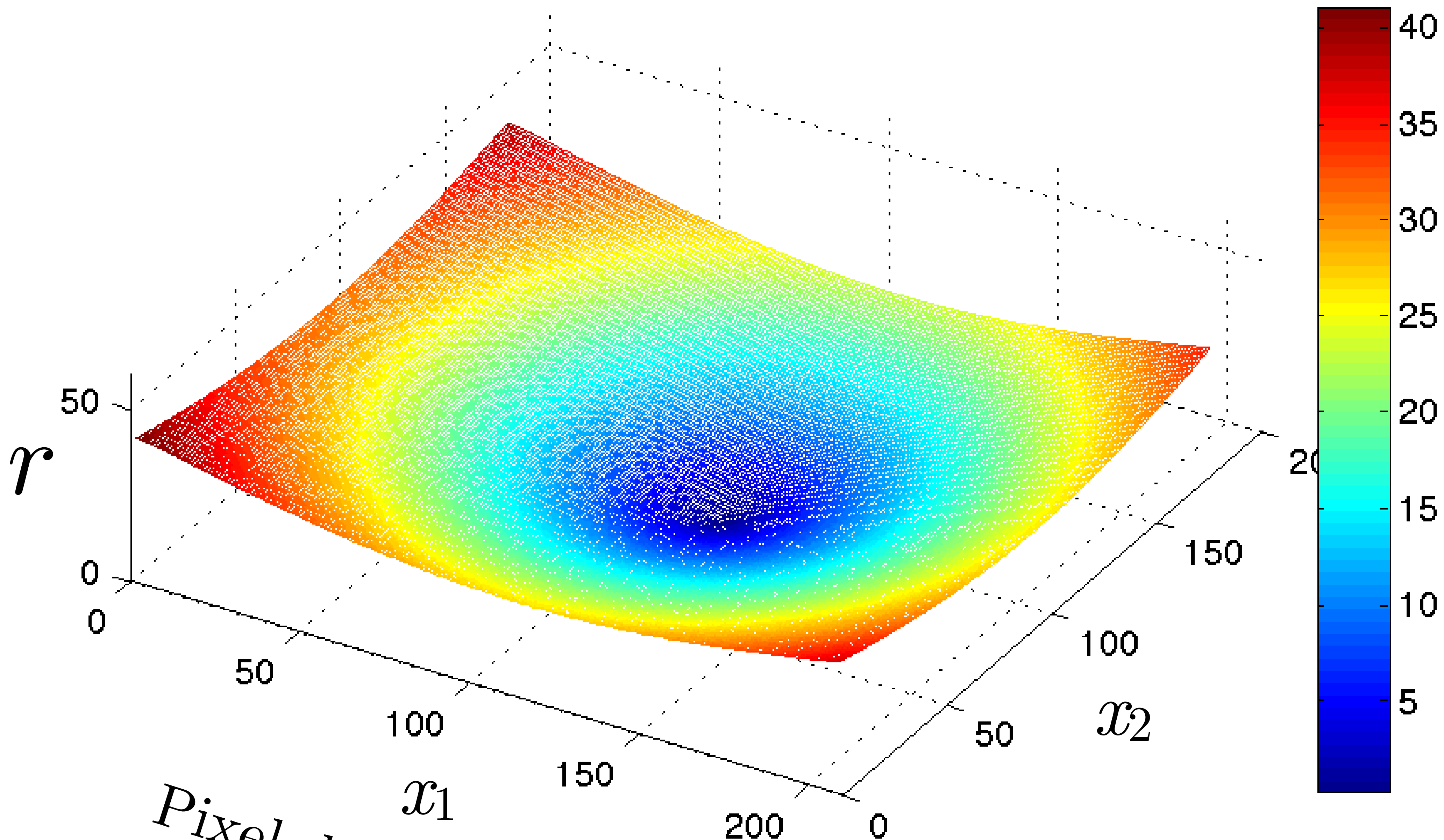

Pixel domain =
object surface

Deflection radius r vs CCD pixel

Radial slope
$=$ local dioptric power

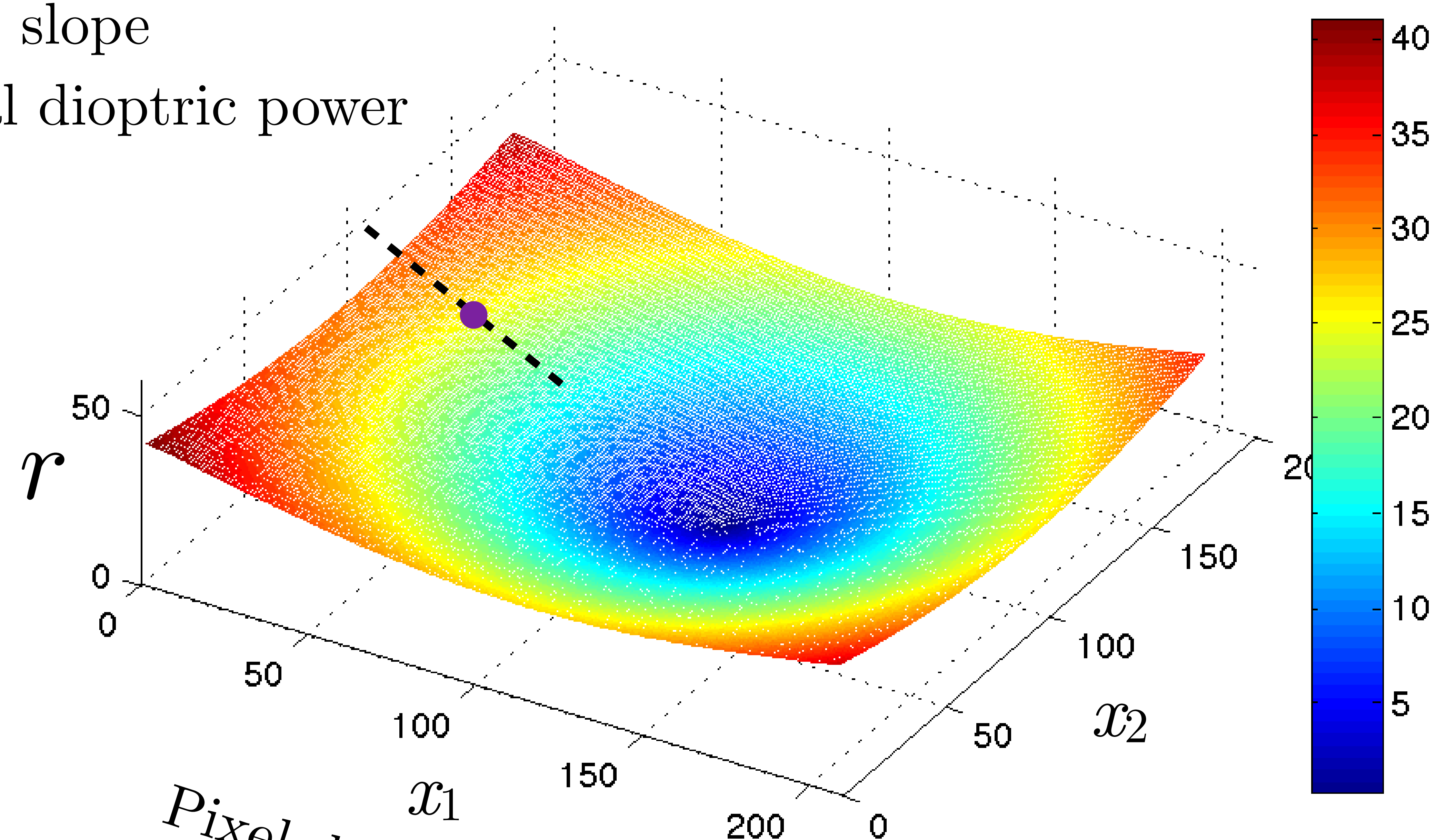

Pixel domain $=$
object surface

Main deflection without reconstruction? 1/2

- $\widehat{\boldsymbol{s}}_k$ characterized by $\widehat{\tau}_k = (\bar{c}^x_k, \bar{c}^y_k)^T$.

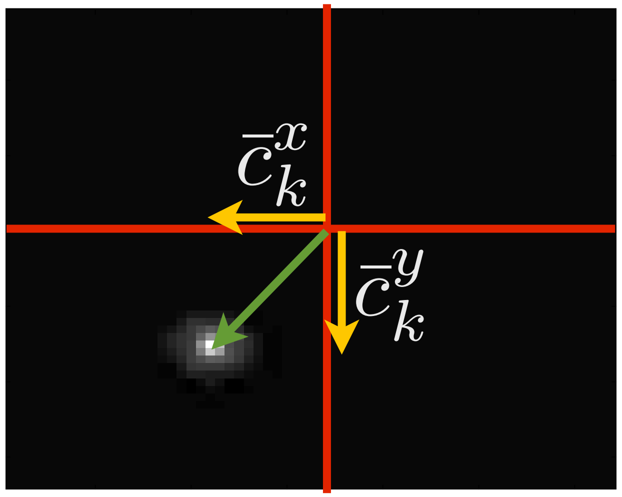

Location of dominant deflection.

- $\boldsymbol{g}^\rho_\tau$: 2D Gaussian 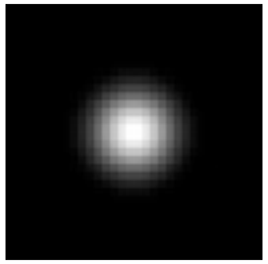

with radius ρ, **translated** by τ.

- Matched filtering $\widehat{\tau}_k = \arg\max_\tau |\langle \widehat{\boldsymbol{s}}_k, \boldsymbol{g}^\rho_\tau \rangle|$.

- Efficiently implemented as convolution

- Can we do something similar in compressive domain?

Main deflection without reconstruction? 2/2

Compressive matched filtering ➠ **Smashed filtering***

$$\boldsymbol{y}_k \in \mathbb{R}^M, \ \ \widetilde{\tau}_k = \arg\max_{\tau} \left|\langle \boldsymbol{\Phi}^T \boldsymbol{y}_k, \boldsymbol{g}^{\rho}_{\tau} \rangle\right|.$$

Thanks to the RIP

$\|\widetilde{\tau}_k - \widehat{\tau}_k\|_2$ averaged over several k

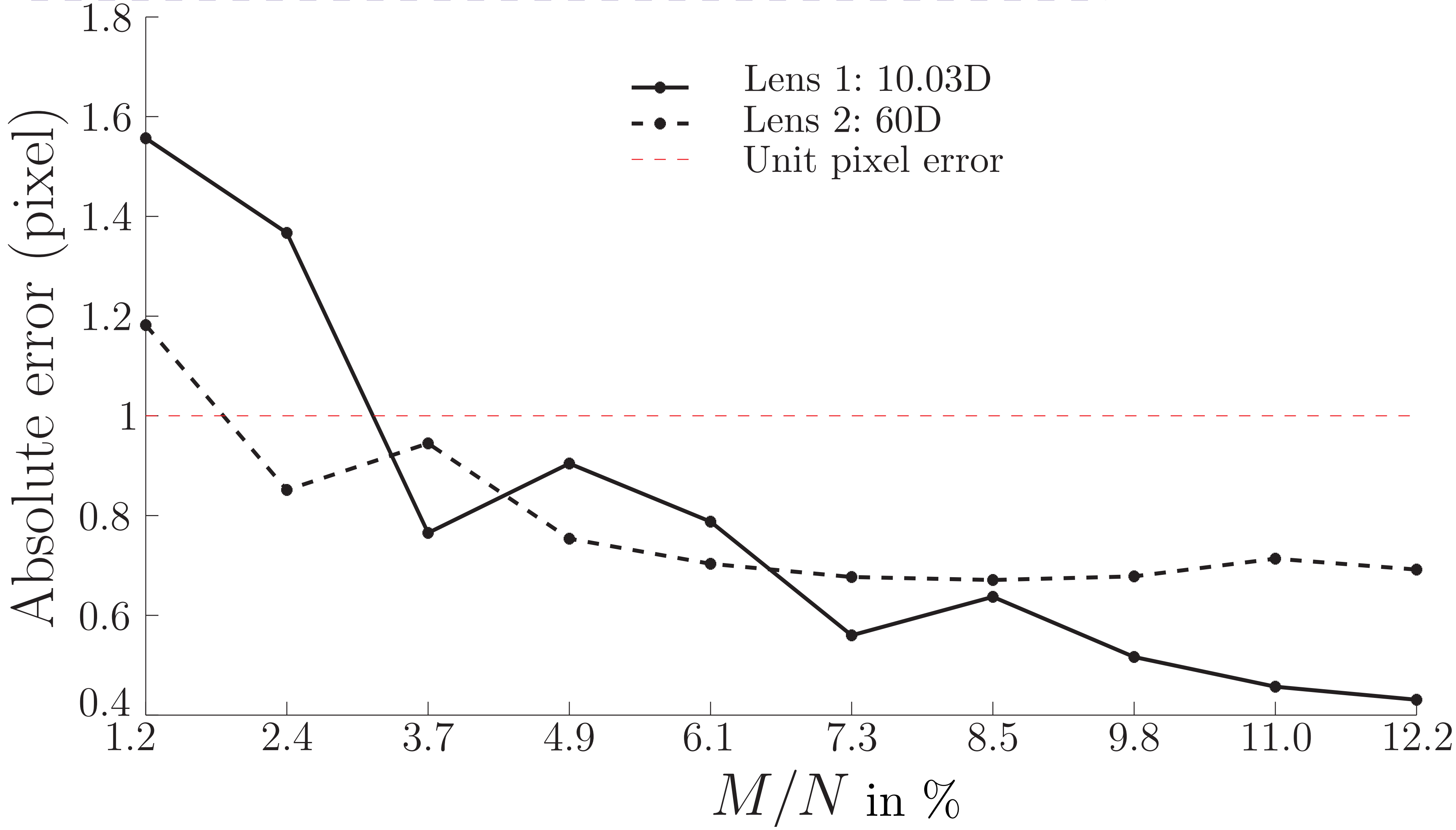

* M. A. Davenport et al., "Signal processing with compressive measurements," IEEE J. Sel. T. Sig. Proc., 2010.

Visualization plot

Plot of each r for CCD pixel:

Multifocal diffractive IOL: 2
Dioptric powers 28D and 30.25D

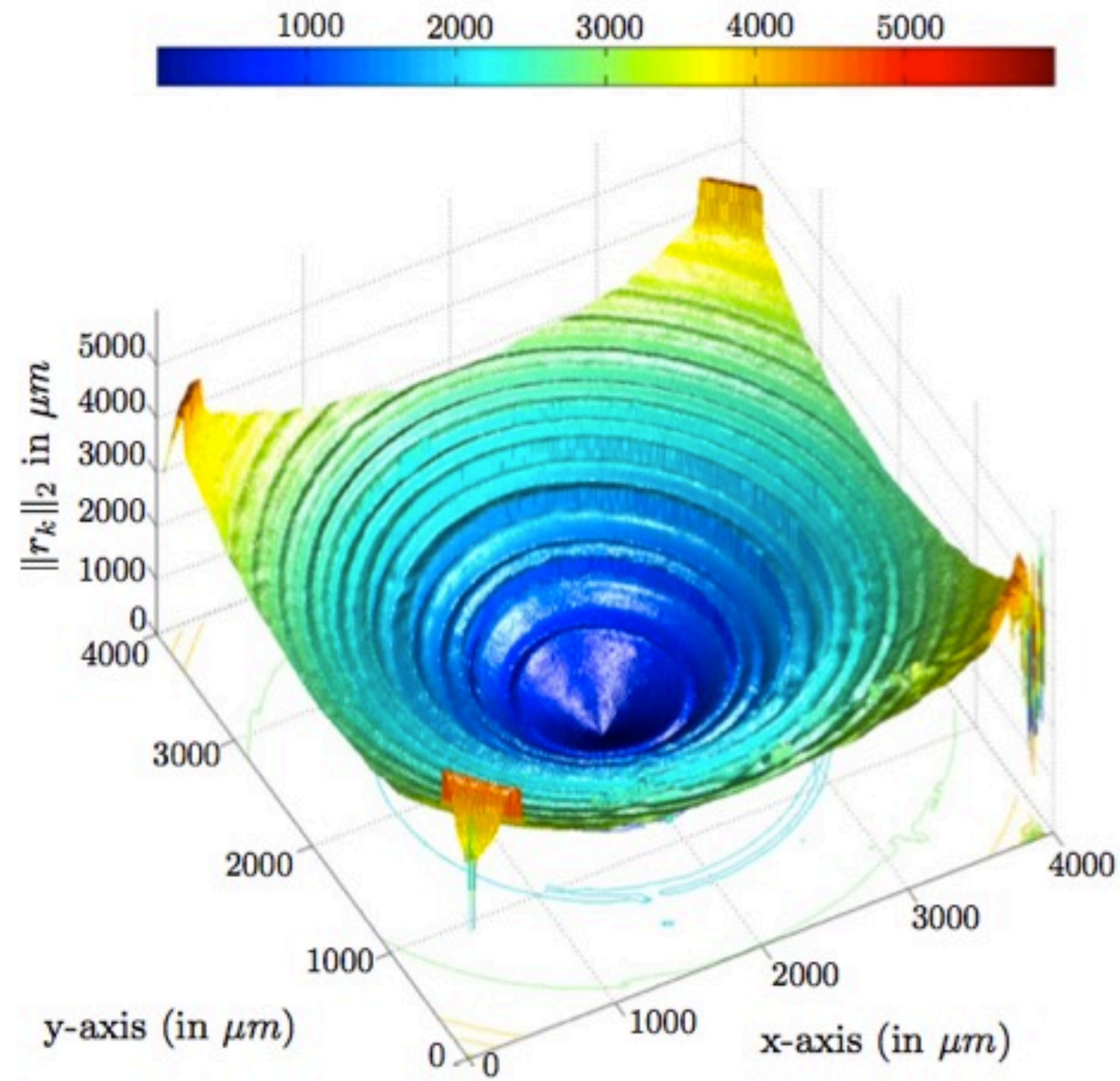

CS estimation, $M/N = 7.63\%$

Visualization plot

Plot of each r for CCD pixel:

Multifocal diffractive IOL: 2 Dioptric powers 28D and 30.25D

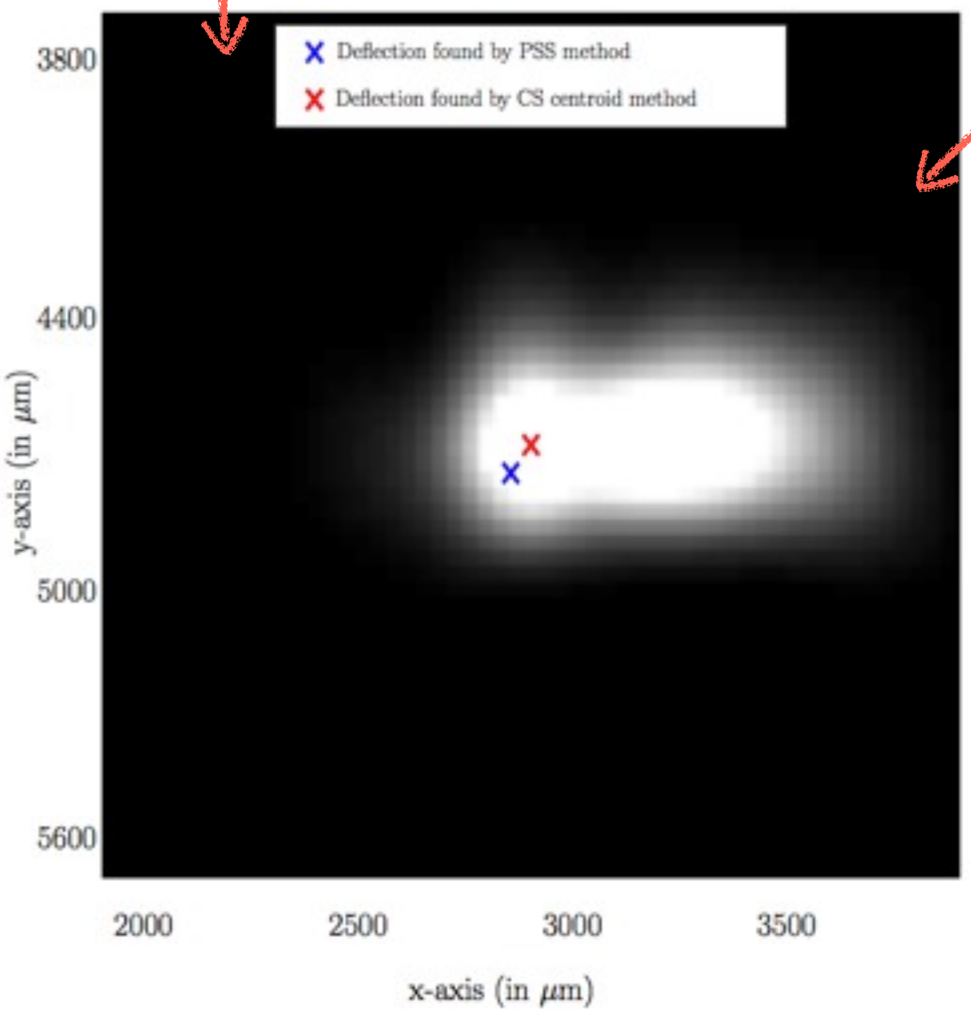

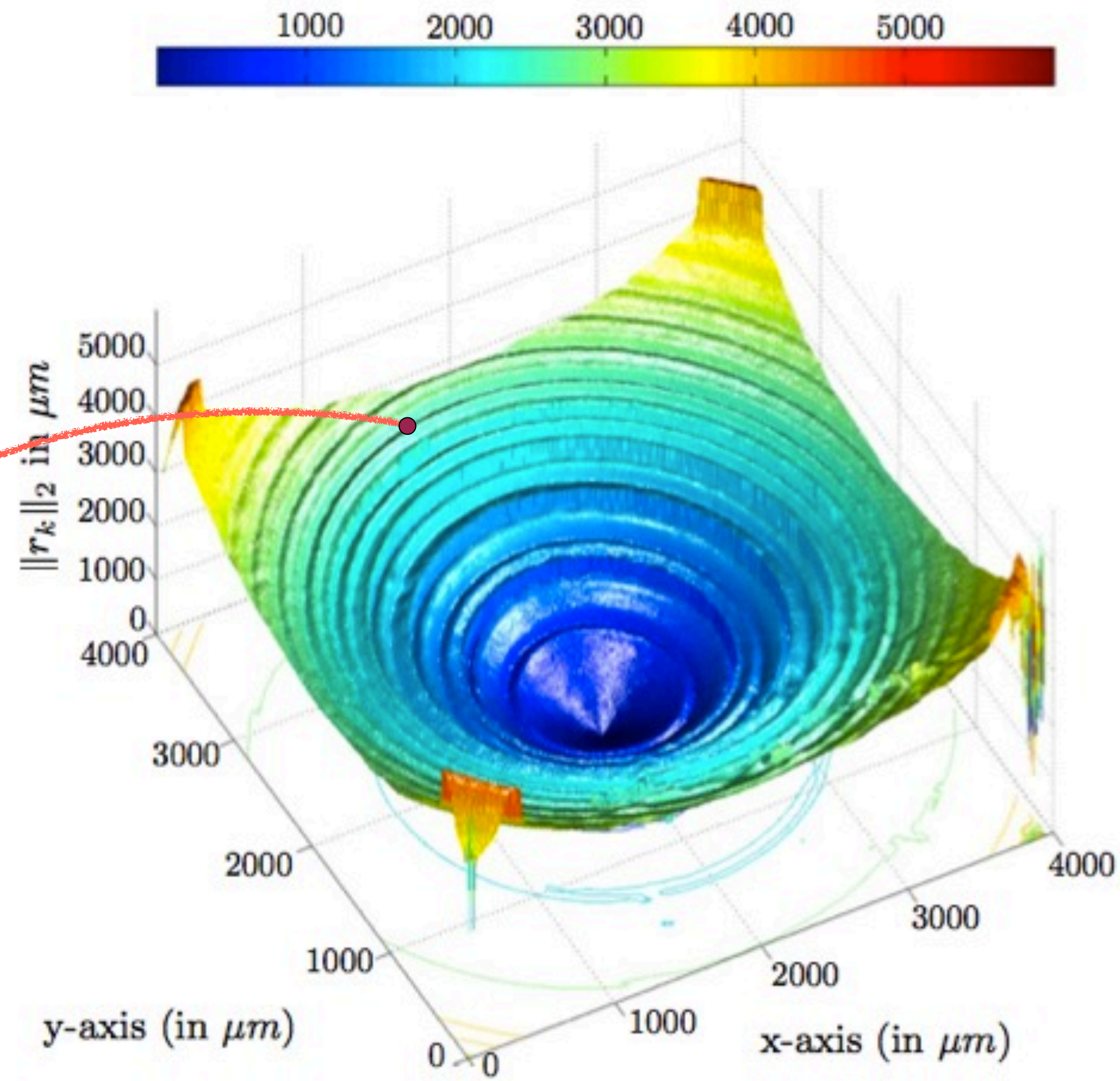

CS estimation, $M/N = 7.63\%$

Summary and further work

- A real world instance of compressive sensing in action ... and its use
- Practical systems pose their own challenges
- Further...
  - Detailed noise modeling + calibration + nonlinearities
  - Multiple-location reconstruction
  - Consideration of system's PSF:

    blind compressive deconvolution

Part III:

Optical Deflectometry

(main contributor: Adriana Gonzalez)

Optical Deflectometric Tomography

Interest

- Optical characterization of (transparent) objects

ODT

- Tomographic Imaging Modality
- Measures light deviation caused by the difference in the object refractive index


Optical fibers

Intraocular lenses


Optical Deflectometric Tomography

Interest

- Optical characterization of (transparent) objects

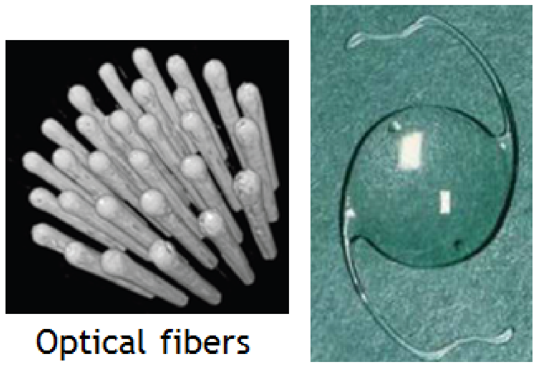

ODT

- Tomographic Imaging Modality
- Measures light deviation caused by the difference in the object refractive index

Tomographic model

$$\mathsf{n}(\boldsymbol{r}) \to \alpha(\tau, \theta)$$

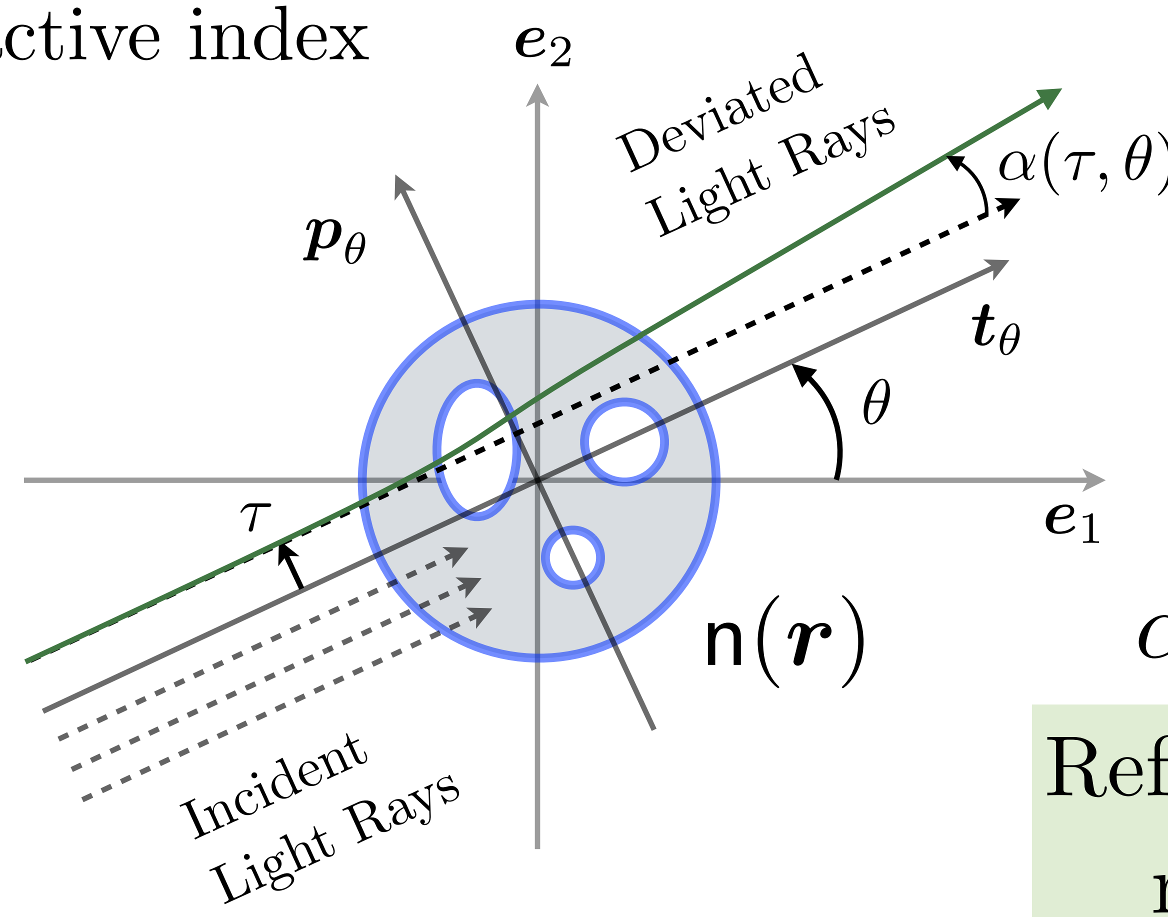

$$\alpha(\tau, \theta) \to \mathsf{n}(\boldsymbol{r})$$

Refractive index map reconstruction !

How to measure light deflections?

- We use our Schlieren Deflectometer (See Part 2)

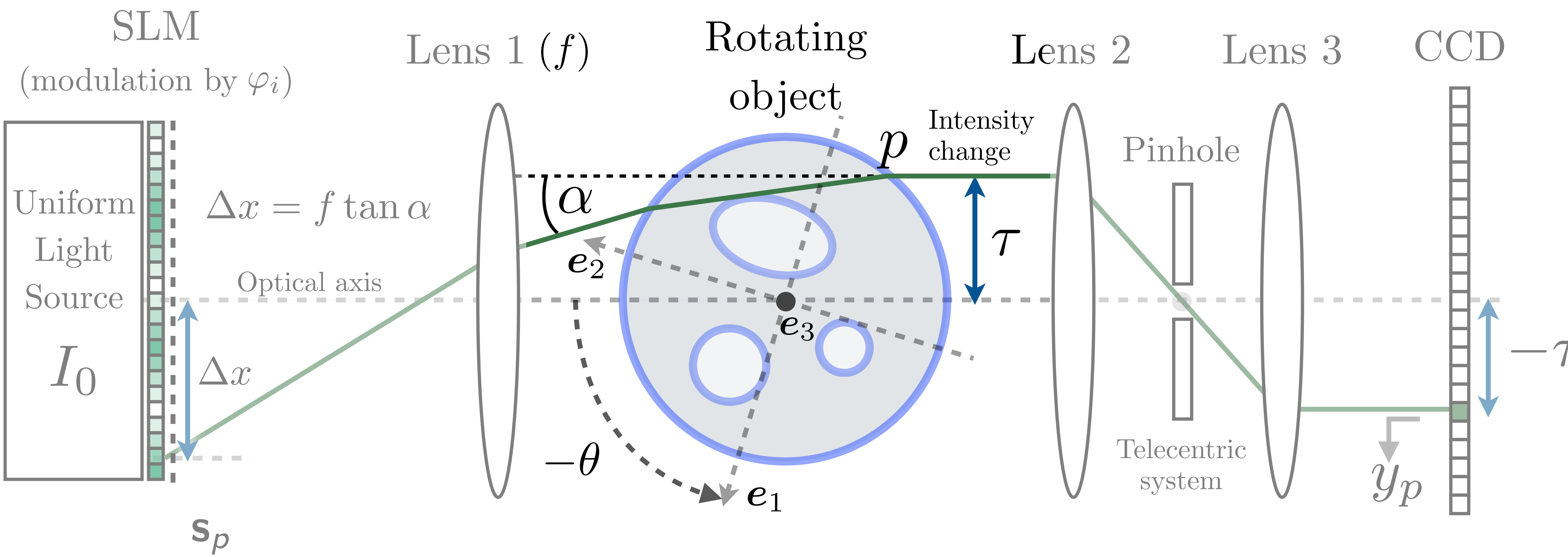

Here: hypothesis of single deflection,
One deflection map for each rotation

Continuous model

Mathematical Model

- Eikonal equation
  $\mathcal{R}$ curved : $\mathbf{r}(s) \to \frac{\mathrm{d}}{\mathrm{d}s}\left(\mathfrak{n}\frac{\mathrm{d}}{\mathrm{d}s}\mathbf{r}(s)\right) = \boldsymbol{\nabla}\mathfrak{n}$
- Approximation
  small $\alpha \to \mathcal{R}$ straight : $\mathbf{r} \cdot \mathbf{p}_\theta = \tau$
  error $< 10\%$
  $\alpha(\tau, \theta) = \sin(\alpha)$

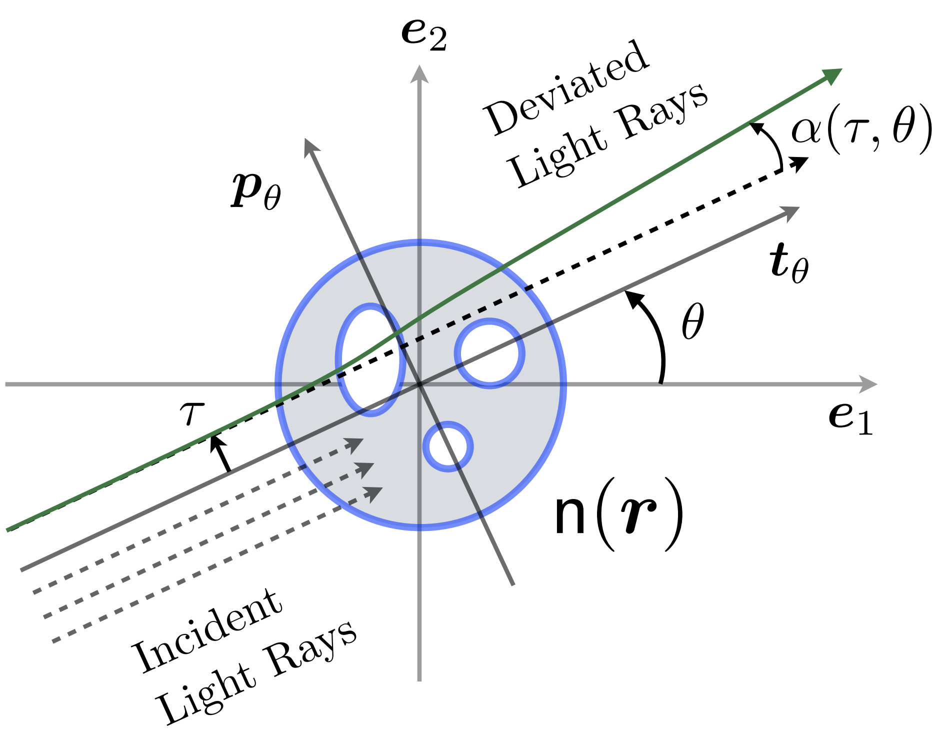

$$\alpha(\tau, \theta) = \frac{1}{\mathfrak{n}_\mathrm{r}} \int_{\mathbb{R}^2} \left(\boldsymbol{\nabla}\mathfrak{n}(\mathbf{r}) \cdot \mathbf{p}_\theta\right)\, \delta(\tau - \mathbf{r} \cdot \mathbf{p}_\theta)\, \mathrm{d}^2\mathbf{r}$$

Continuous model

Mathematical Model

- Eikonal equation
  $\mathcal{R}$ curved : $\mathbf{r}(s) \to \frac{\mathrm{d}}{\mathrm{d}s}\big(\mathfrak{n}\frac{\mathrm{d}}{\mathrm{d}s}\mathbf{r}(s)\big) = \boldsymbol{\nabla}\mathfrak{n}$
- Approximation
  small $\alpha \to \mathcal{R}$ straight : $\mathbf{r}\cdot\mathbf{p}_\theta = \tau$
  error $< 10\%$
  $\alpha(\tau,\theta) = \sin(\alpha)$

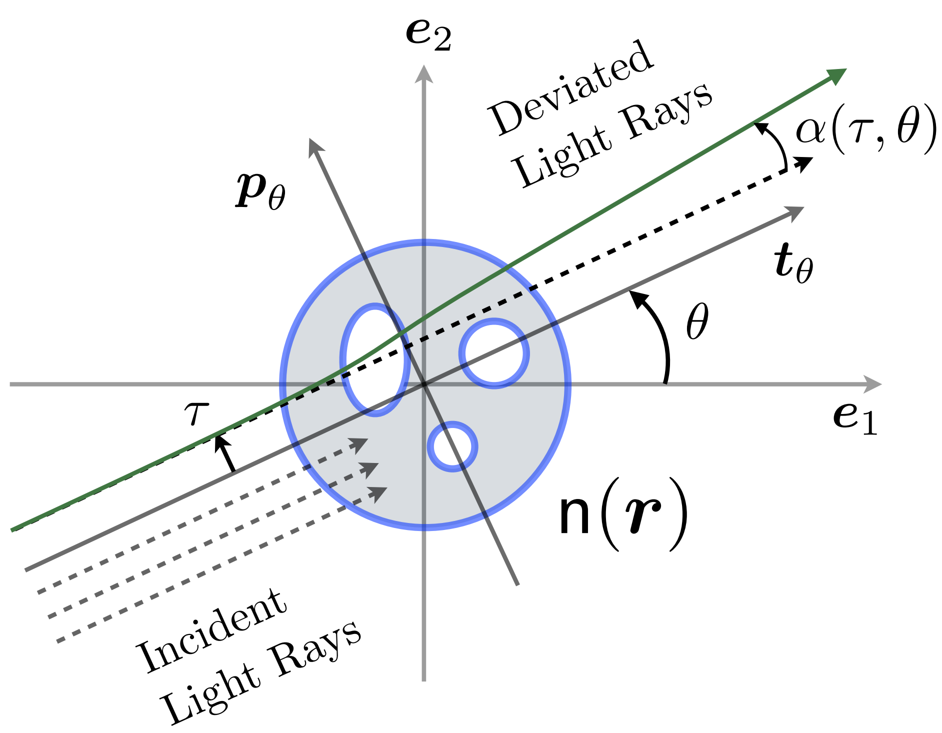

$$\alpha(\tau,\theta) = \frac{1}{\mathfrak{n}_{\mathrm{r}}}\int_{\mathbb{R}^2}\big(\boldsymbol{\nabla}\mathfrak{n}(\mathbf{r})\cdot\mathbf{p}_\theta\big)\;\delta(\tau-\mathbf{r}\cdot\mathbf{p}_\theta)\,\mathrm{d}^2\mathbf{r}$$

Deflectometric Central Slice Theorem:

$$y(\omega,\theta) := \int_{\mathbb{R}}\alpha(\tau,\theta)\,e^{-2\pi i\tau\omega}\mathrm{d}\tau \;=\; \frac{2\pi i\omega}{\mathfrak{n}_{\mathrm{r}}}\,\widehat{\mathfrak{n}}(\omega\,\mathbf{p}_\theta)$$

$\widehat{\mathfrak{n}}(\omega\,\mathbf{p}_\theta)$: 2-D Fourier transform of $\widehat{\mathfrak{n}}$ in Polar grid

Discrete Forward Model

$$y = \frac{2\pi i(\delta r)^2}{\mathfrak{n}_{\mathrm{r}}}\,\mathrm{diag}(\omega_{(1)},\cdots,\omega_{(M)})\,\widehat{\mathfrak{n}}$$

$$\Downarrow$$

$$\mathbf{y} = \mathbf{D}\mathbf{F}\mathfrak{n} + \boldsymbol{\eta}$$

- $\mathfrak{n} \in \mathbb{R}^N$; Cartesian grid of $N = N_0^2$ pixels; sampling: δr
- $\mathbf{y} \in \mathbb{R}^M$; Polar grid of $M = N_\tau N_\theta$ pixels; sampling: $\delta\tau$, $\delta\theta$
- $\mathbf{D}$: $\frac{2\pi i(\delta r)^2}{\mathfrak{n}_{\mathrm{r}}}\,\mathrm{diag}(\omega_{(1)},\cdots,\omega_{(M)}) \in \mathbb{C}^{M\times M}$
- $\mathbf{F} \in \mathbb{C}^{M\times N}$: Non-equispaced Fourier Transform (NFFT) [4]
- $\boldsymbol{\eta} \in \mathbb{C}^M$: numerical computations, model discretization, model discrepancy, observation noise

[4] J. Keiner et al. (2009)

ODT vs. AT

$$\mathbf{y} = \mathbf{D}\mathbf{F}\mathfrak{n} + \boldsymbol{\eta}$$

- Main difference: Operator **D**
- Without noise $\boldsymbol{\eta} \to$ classical tomographic model

$$\tilde{\mathbf{y}} = \mathbf{D}^{-1}\mathbf{y} = \mathbf{F}\mathfrak{n}$$

- For $\boldsymbol{\eta} \neq 0 \to$ Not a classical tomographic model
  - $\boldsymbol{\eta}$: AWGN $\to \mathbf{D}^{-1}\boldsymbol{\eta}$ not homoscedastic

ODT vs. AT

Observation: 1-D FT of sinograms along the τ direction

Absorption Tomography

Optical Deflection Tomography

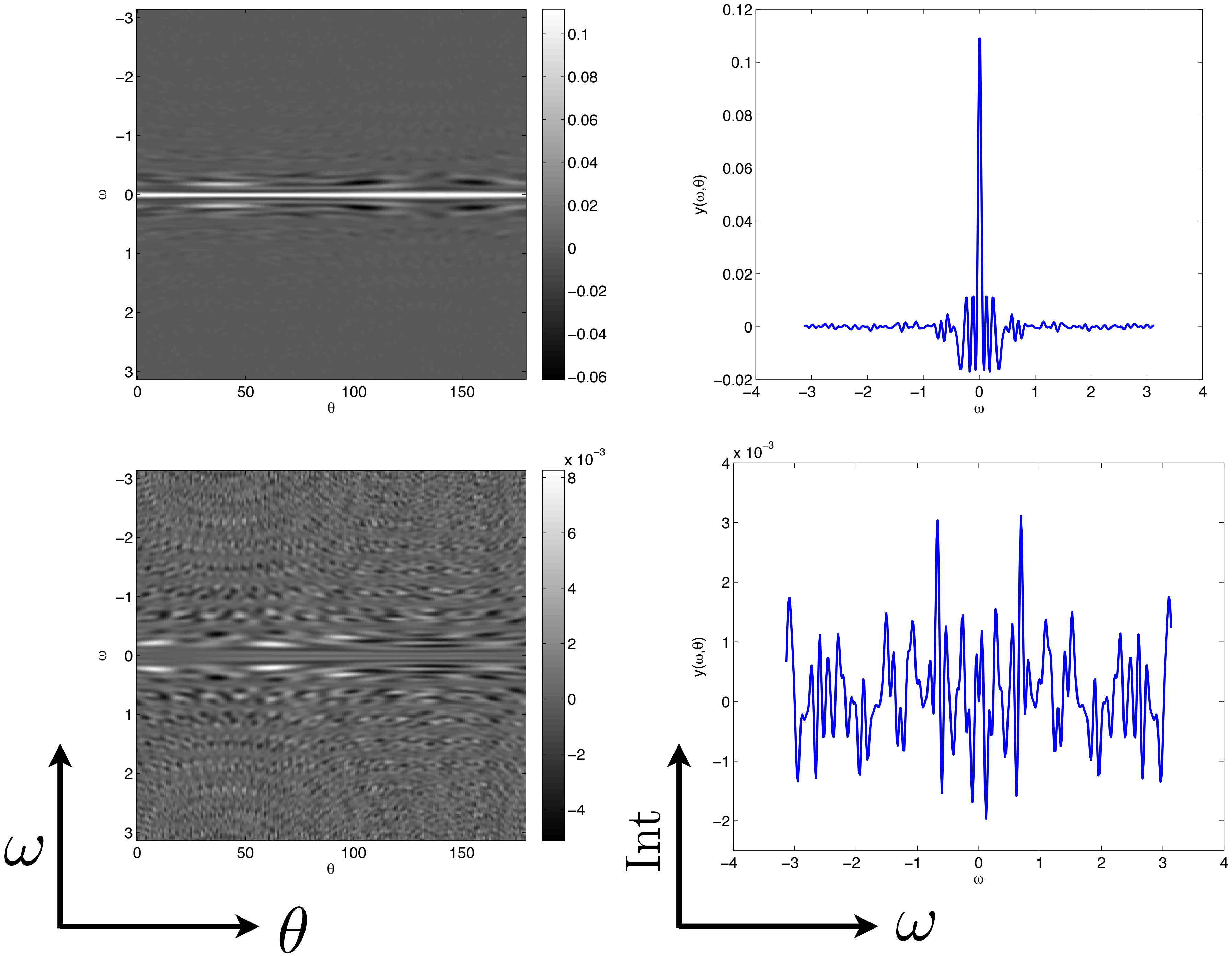

Standard Reconstruction Methods

$$\mathbf{y} = \boldsymbol{\Phi}\mathfrak{n} + \eta = \mathbf{DF}\mathfrak{n} + \eta$$

1. **Filtered Back Projection**
   - Analytical method
   - Solution $\tilde{\mathfrak{n}}_{\mathrm{FBP}}$:
     - Filtering the tomographic projections
       AT: ramp filter; ODT: Hilbert filter
     - Backprojecting in the spatial domain by angular integration

2. **Minimum Energy Reconstruction**

$$\tilde{\mathfrak{n}}_{\mathrm{ME}} = \boldsymbol{\Phi}^{\dagger}\mathbf{y} = \boldsymbol{\Phi}^{*}(\boldsymbol{\Phi}\boldsymbol{\Phi}^{*})^{-1}\mathbf{y} \qquad \equiv \qquad \tilde{\mathfrak{n}}_{\mathrm{ME}} = \arg\min_{\mathbf{u}\in\mathbb{R}^N} \|\mathbf{u}\|_2 \text{ s.t. } \mathbf{y} = \boldsymbol{\Phi}\mathbf{u}$$

Problems:
- Noise
- Compressiveness $\Rightarrow M(N_\theta) < N$
  $\Rightarrow$ ill-posed problem

Solution:
Regularization

Sparsity prior

Heterogeneous transparent materials with slowly varying refractive index separated by sharp interfaces

Intraocular lenses

Optical fibers

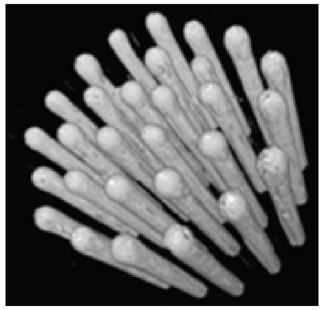

TV and BV promote the perfect "cartoon shape" model

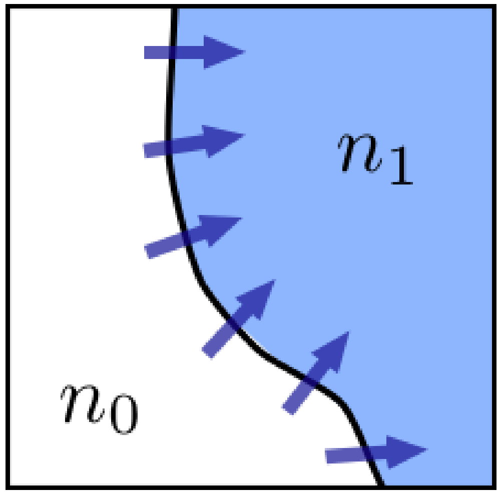

"Sparse" gradient

$\Downarrow$

Small Total Variation norm

$$\|\mathfrak{n}\|_{\mathrm{TV}} := \|\nabla\mathfrak{n}\|_{2,1}$$

Other priors

- Positive RIM

  $\Rightarrow \mathfrak{n} \succeq 0$ (no metamaterial here ;-)

- The object is completely contained in the image. Pixels in the border are set to zero in order to guarantee uniqueness of the solution.

  $\Rightarrow \mathfrak{n}|_{\delta\Omega} = 0$ (up to an intensity shift)

  SOLUTION UNIQUENESS

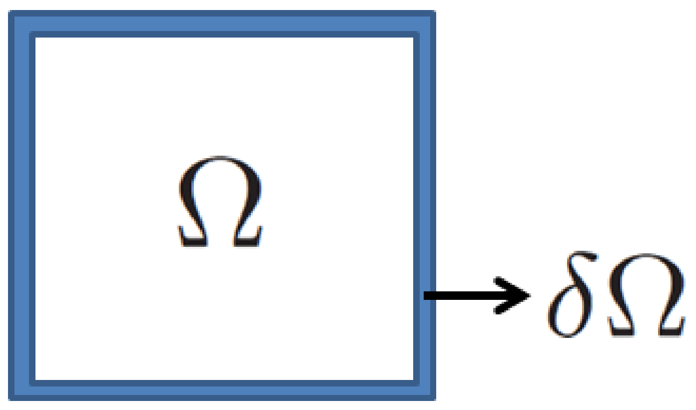

TV-ℓ_2 reconstruction and Noise

$$\mathbf{y} = \mathbf{\Phi}\mathfrak{n} + \boldsymbol{\eta} = \mathbf{D}\mathbf{F}\mathfrak{n} + \boldsymbol{\eta}$$

TV-ℓ_2 Reconstruction

$$\tilde{\mathfrak{n}}_{\mathrm{TV}-\ell_2} = \operatorname*{arg\,min}_{\mathbf{u}\in\mathbb{R}^N} \|\mathbf{u}\|_{\mathrm{TV}} \ \text{ s.t. } \ \|\mathbf{y} - \mathbf{\Phi}\mathbf{u}\|_2 \leq \varepsilon, \ \mathbf{u} \succeq 0, \ \mathbf{u}_{\partial\Omega} = 0$$

Noise

- Observation noise $\rightarrow \sigma^2_{\mathrm{obs}}$
- Modeling error $\rightarrow$ ray tracing with Snell law $\approx 10\%$
- Interpolation noise $\rightarrow$ NFFT error (very small)

$+$ Reconstruction using CP algorithm [5] expanded in a product space

[5] A. Chambolle and T. Pock. Journal of Mathematical Imaging and Vision. (2011)

Synthetic Results

- Compressiveness and noise robustness

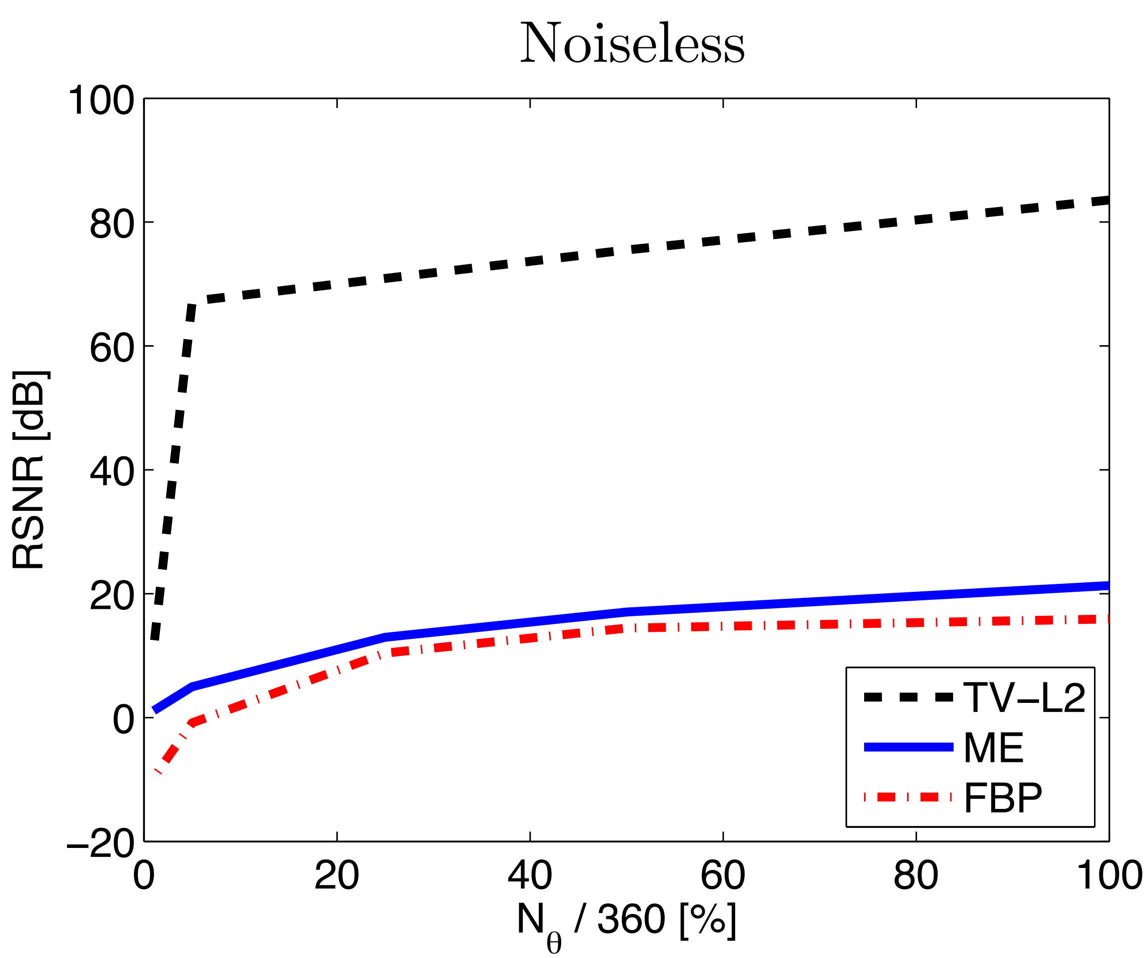

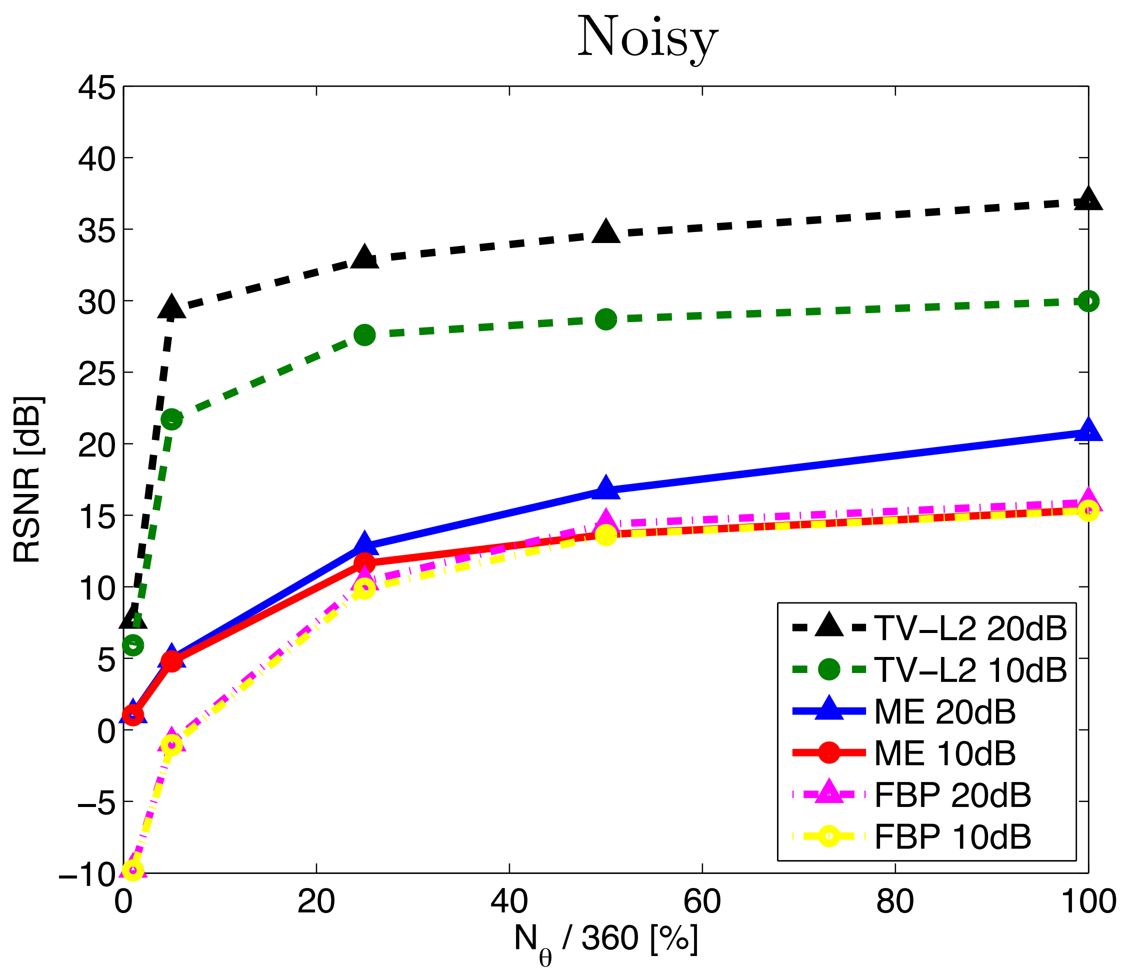

$$\mathrm{MSNR} = 20\log_{10}\frac{\|\boldsymbol{\Delta}\|_2}{\|\boldsymbol{\eta}\|_2} \qquad \mathrm{RSNR} = 20\log_{10}\frac{\|\mathfrak{n}\|_2}{\|\mathfrak{n}-\tilde{\mathfrak{n}}\|_2}$$

Synthetic Results

- No measurement noise (MSNR $= \infty$)
- $N_\theta/360 = 25\%$

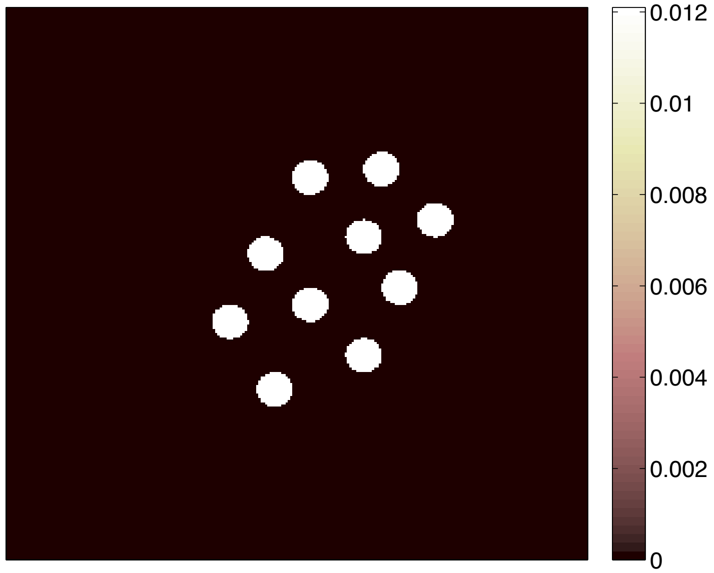

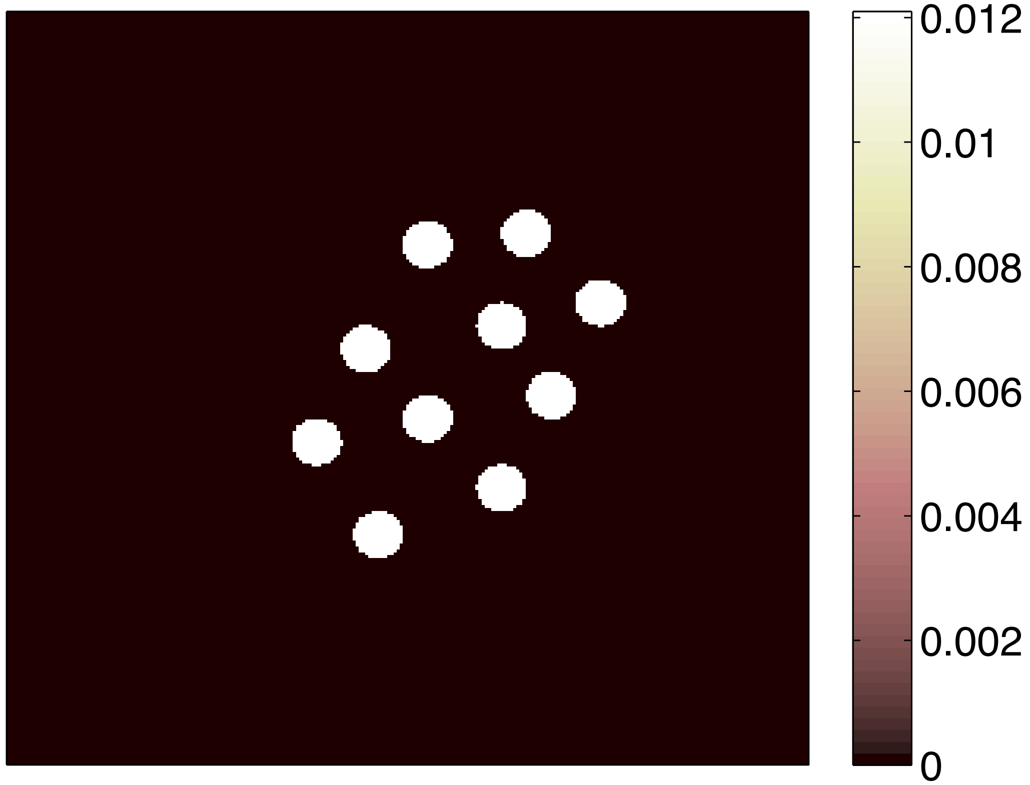

$\tilde{\mathbf{n}}_{\mathrm{TV}-\ell_2}$: RSNR $=$ 71dB

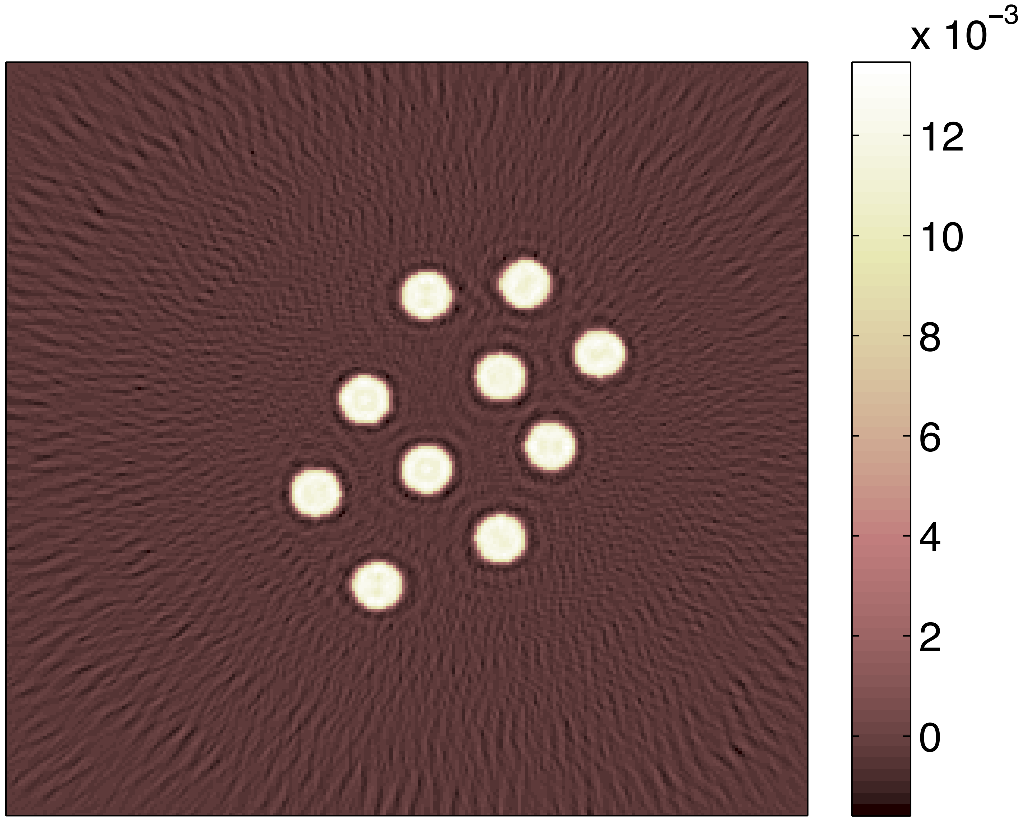

$\tilde{\mathbf{n}}_{\mathrm{ME}}$: RSNR $=$ 13dB

Synthetic Results

- No measurement noise ($\text{MSNR} = \infty$)
- $N_\theta/360 = 5\%$

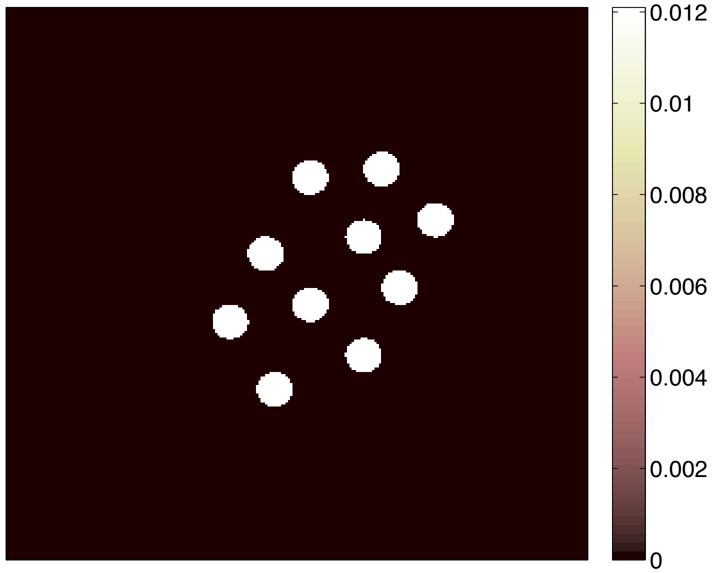

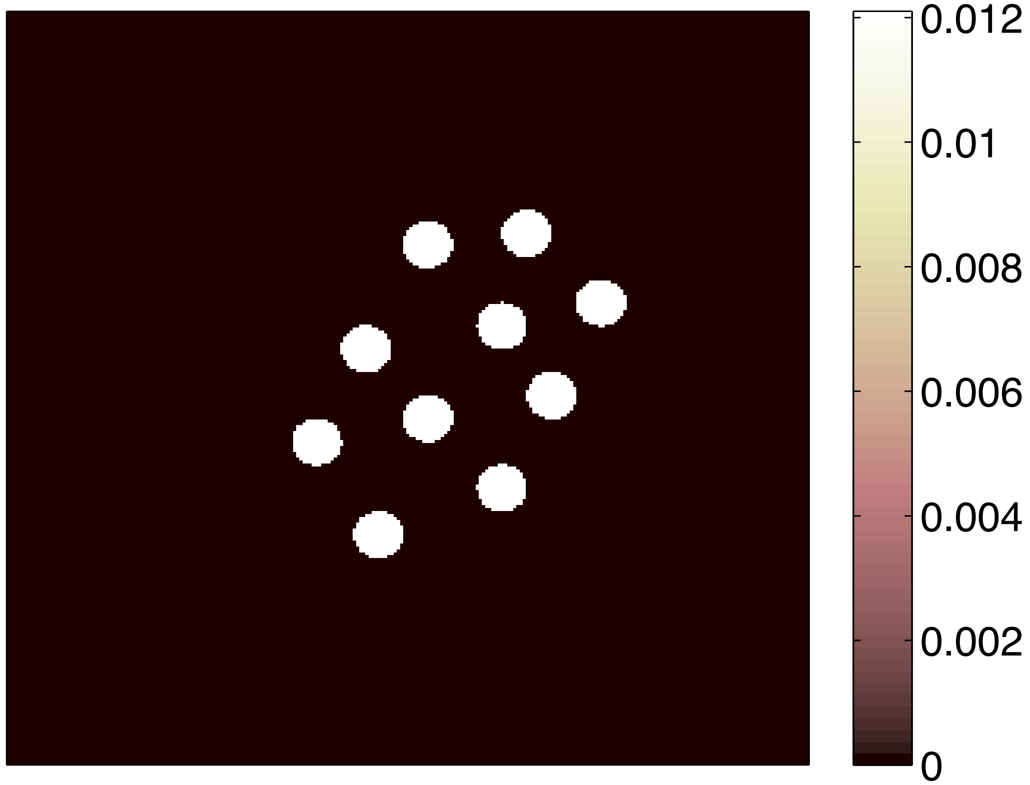

$\tilde{\mathfrak{n}}_{\mathrm{TV}-\ell_2}$: RSNR = 67dB

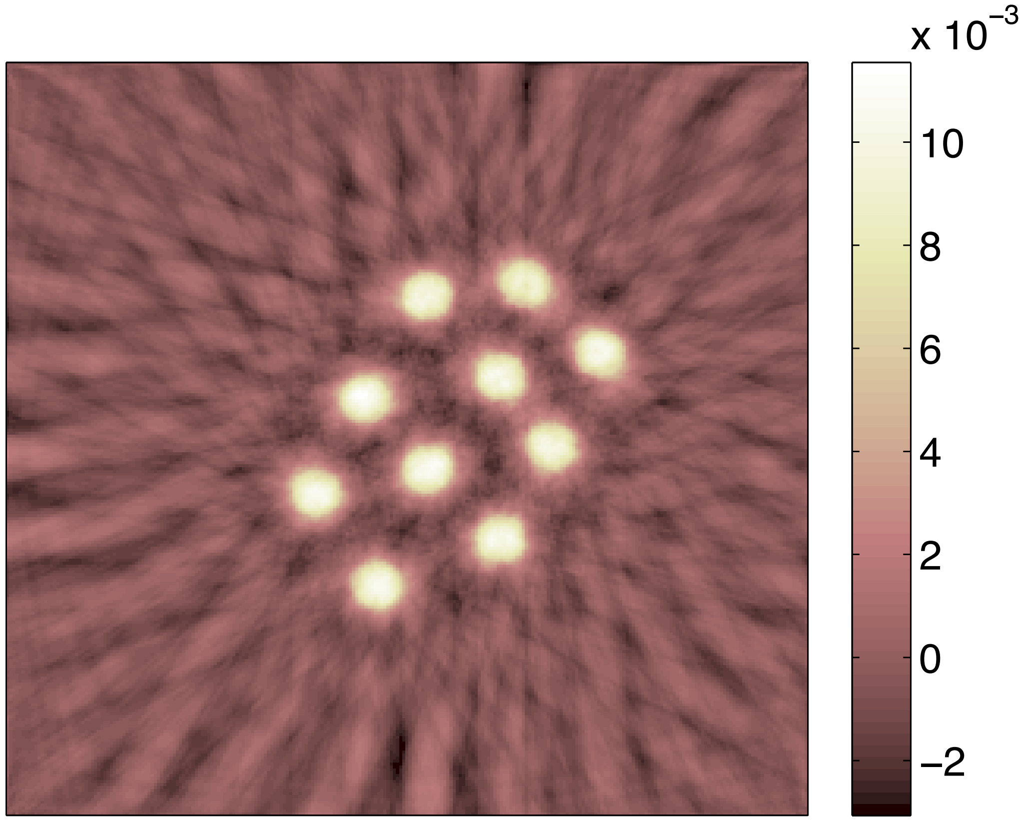

$\tilde{\mathfrak{n}}_{\mathrm{ME}}$: RSNR = 5dB

Experimental Results

- Bundle of 10 fibers immersed in an optical fluid
- MSNR $\approx$ 10dB
- $N_\theta = 60 \Rightarrow N_\theta/360 = 17\%$

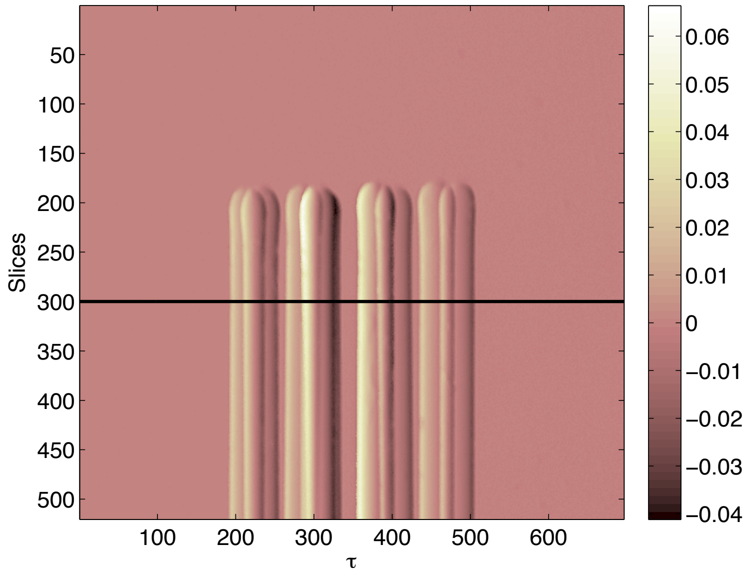

Experimental Results

- Bundle of 10 fibers immersed in an optical fluid
- MSNR $\approx$ 10dB
- $N_\theta = 60 \Rightarrow N_\theta/360 = 17\%$

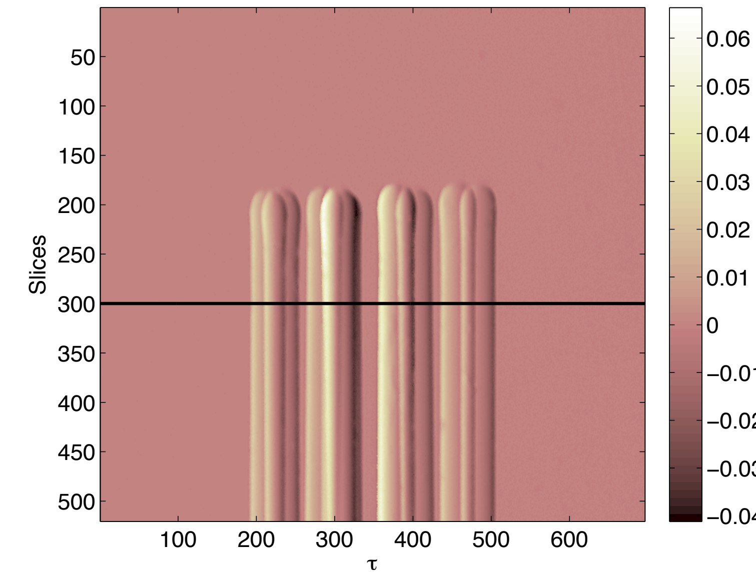

ME

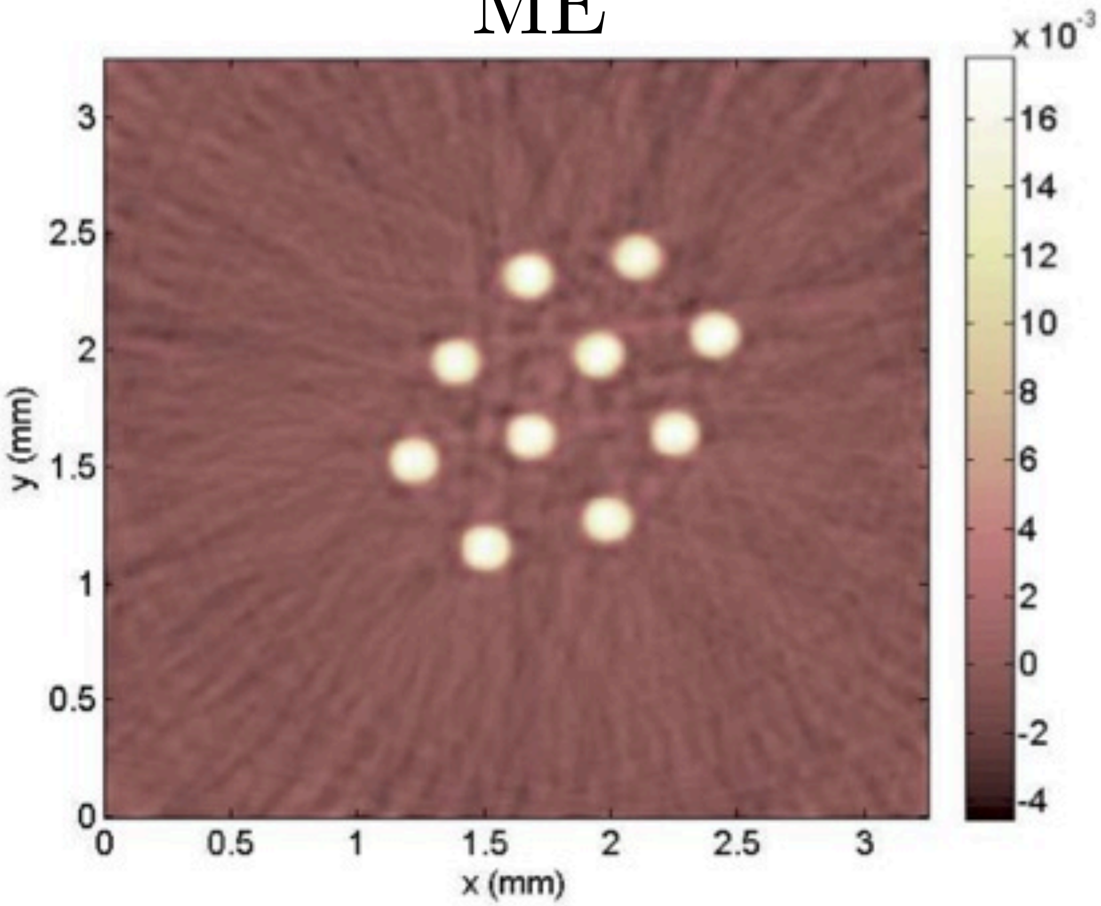

TV-L2

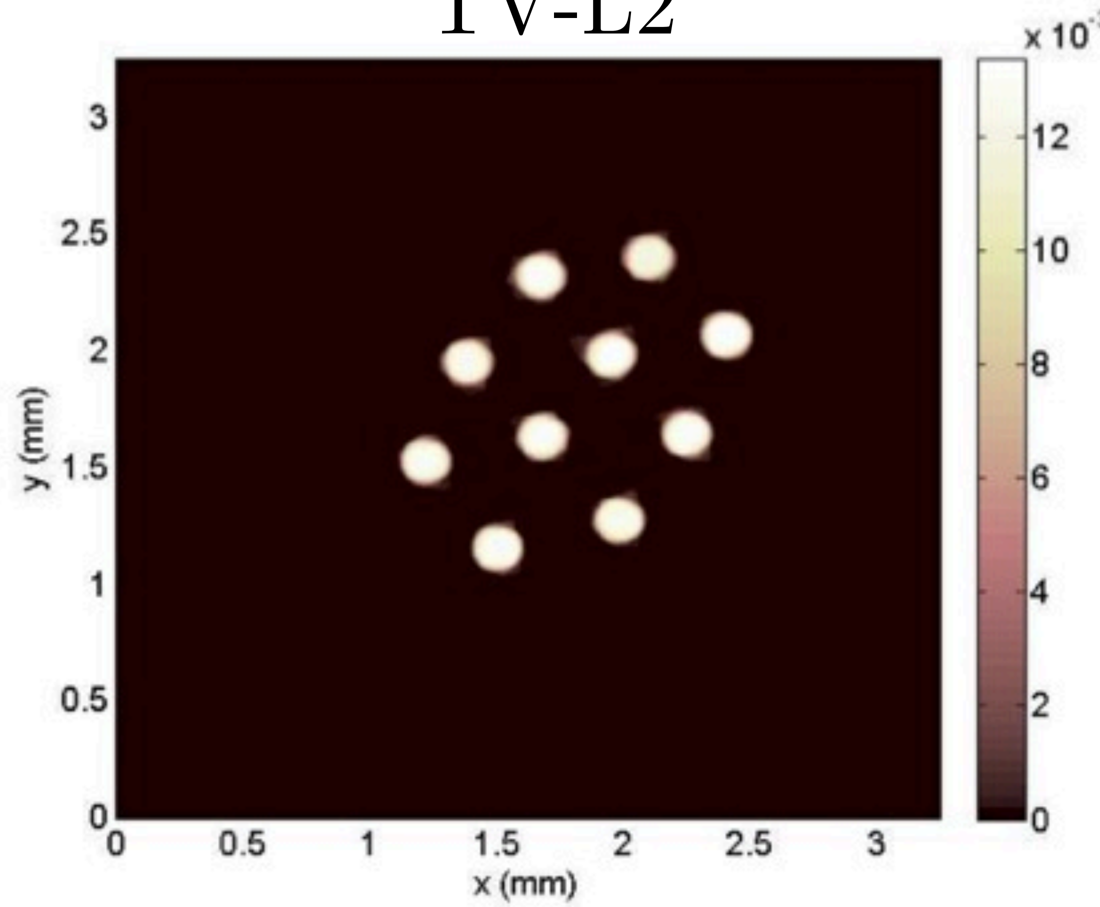

Experimental Results

- Bundle of 10 fibers immersed in an optical fluid
- MSNR $\approx$ 10dB
- $N_\theta = 60 \Rightarrow N_\theta/360 = 17\%$

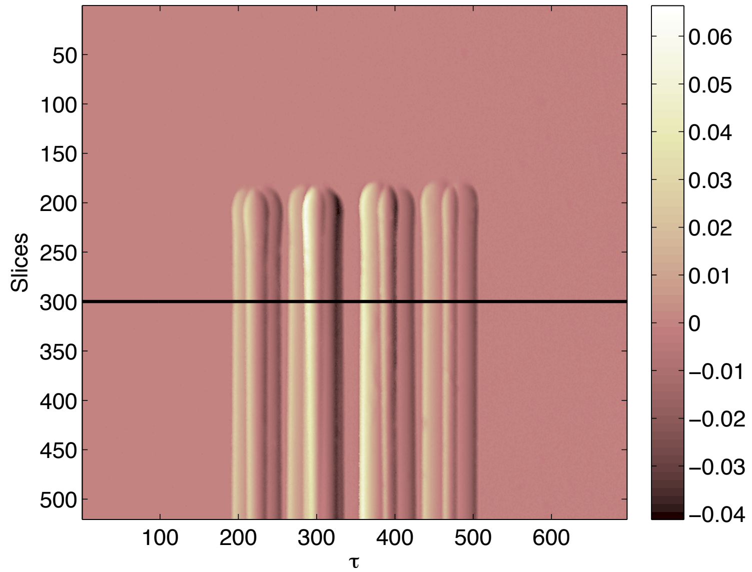

ME

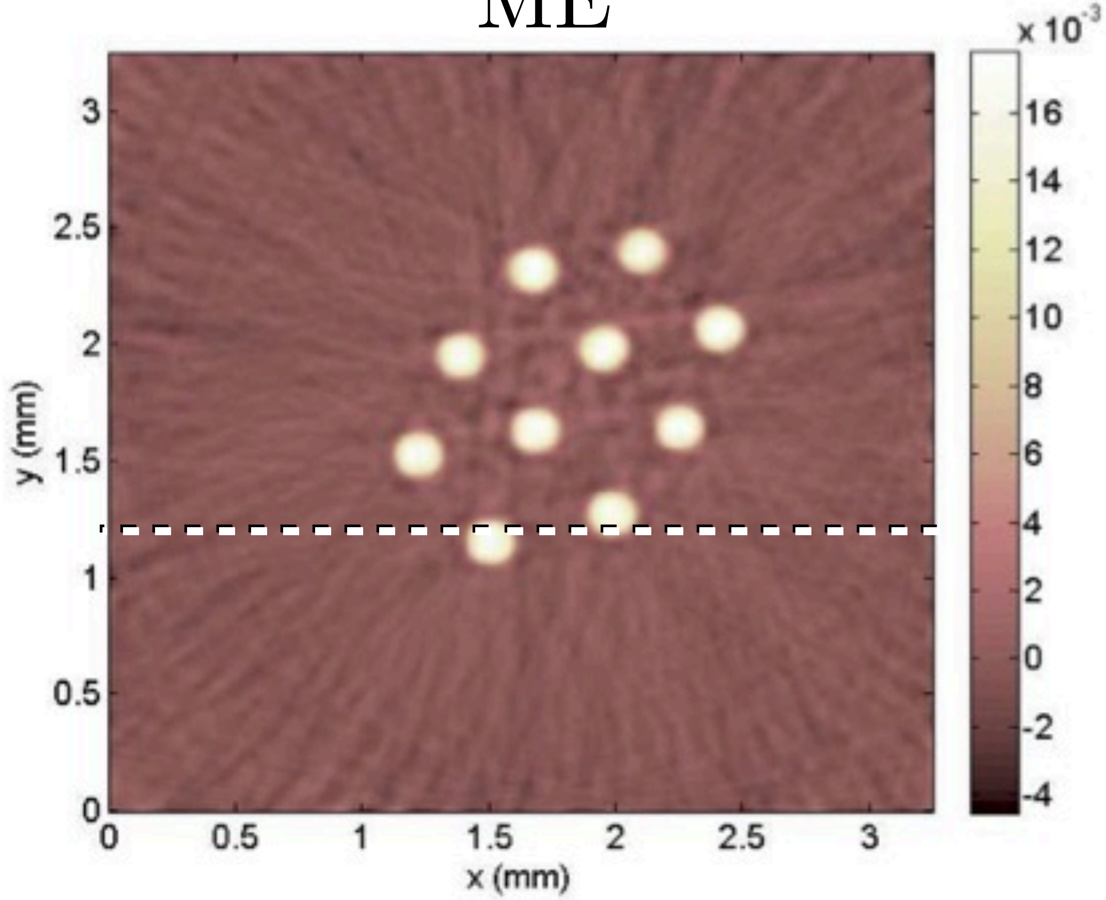

TV-L2

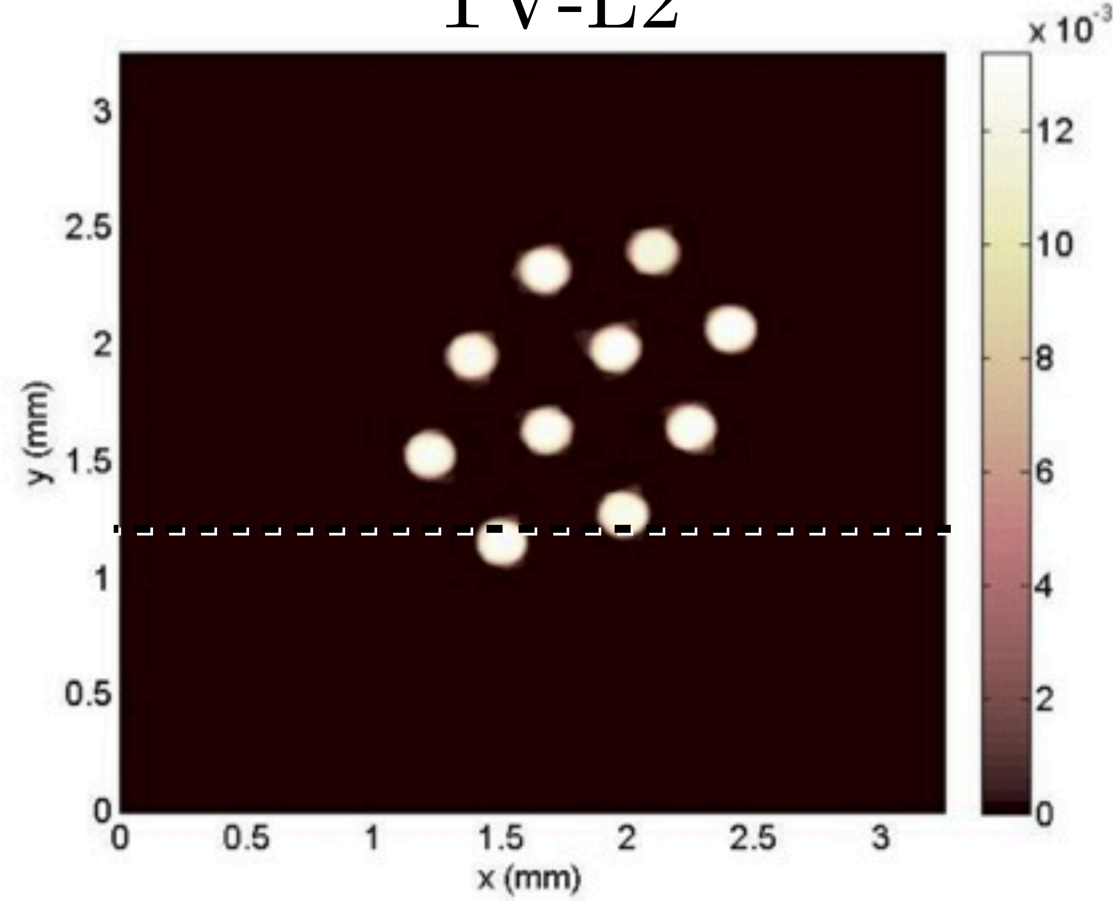

Experimental Results

- Bundle of 10 fibers immersed in an optical fluid
- MSNR $\approx$ 10dB
- $N_\theta = 60 \Rightarrow N_\theta/360 = 17\%$

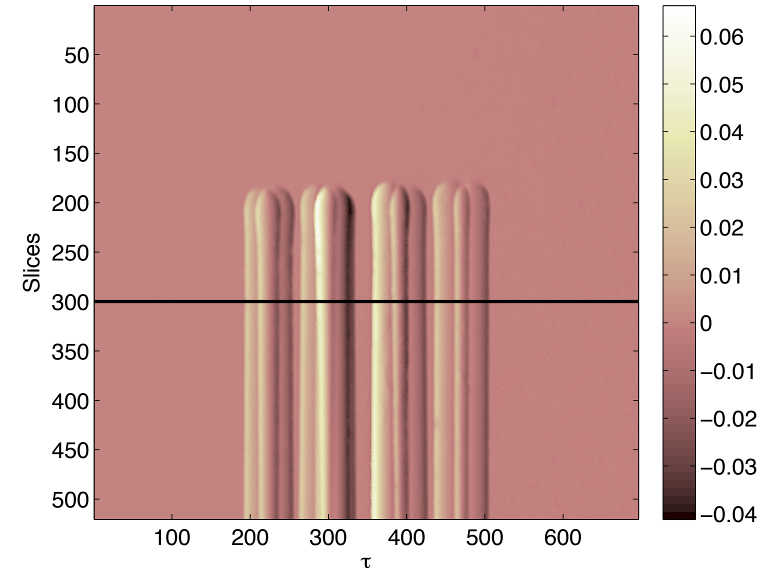

ME

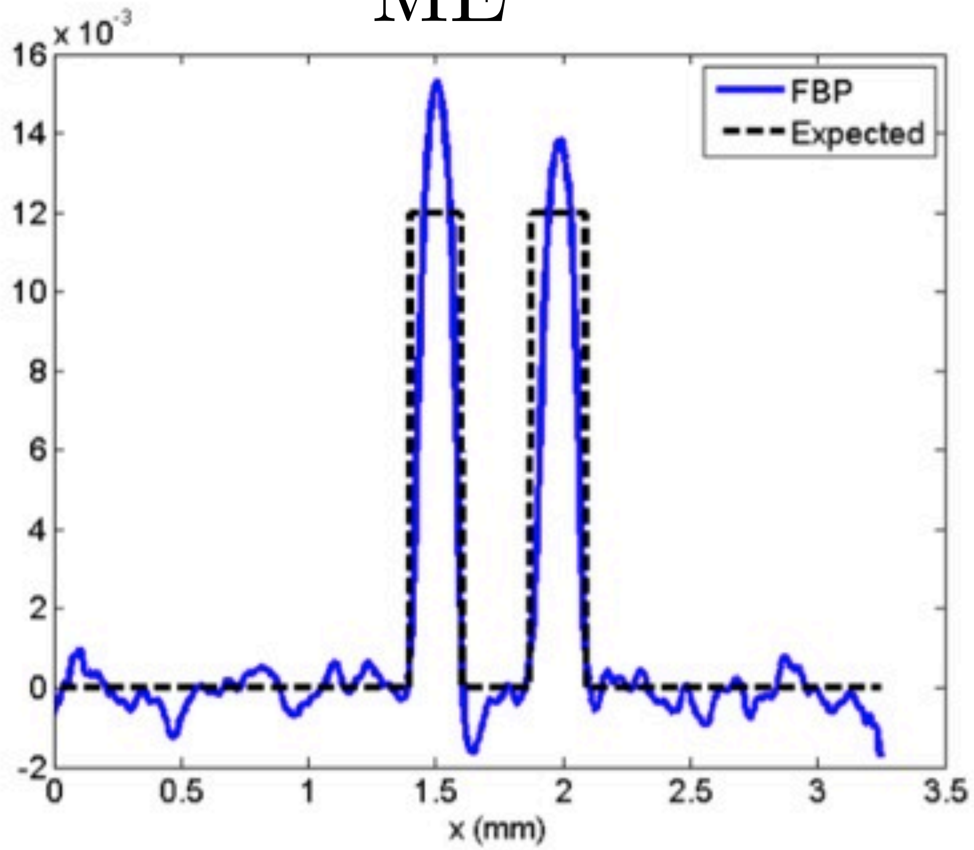

TV-L2

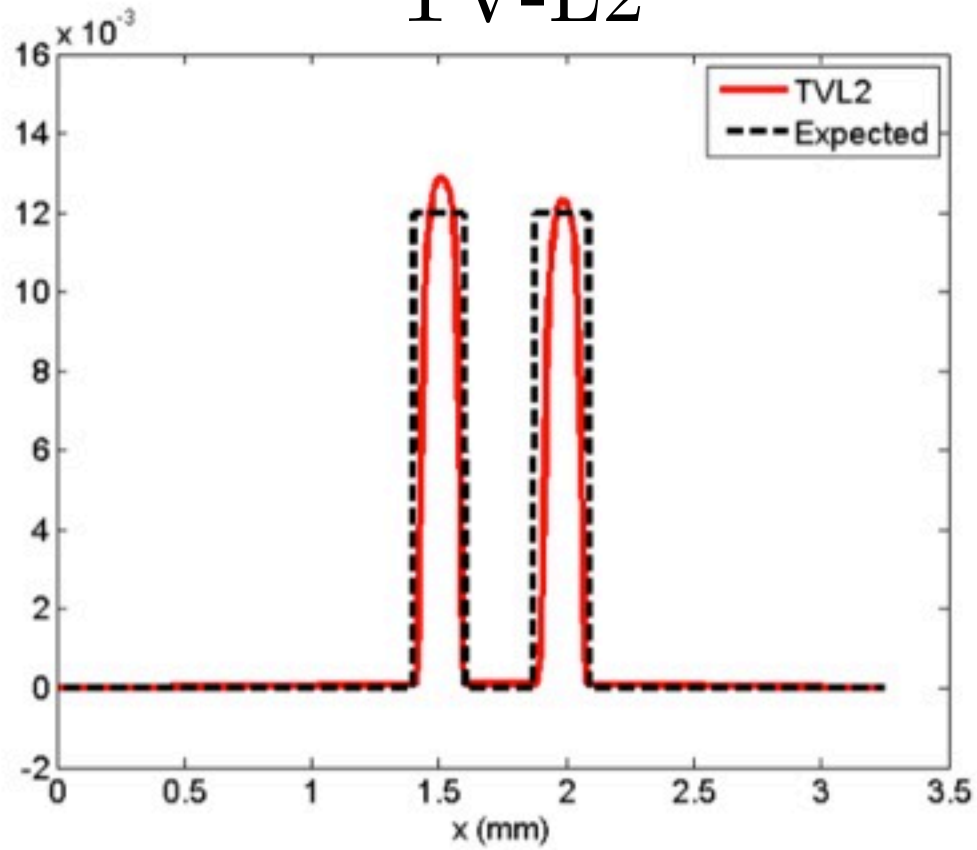

Summary and further work (1/2)

- Optical Deflectometry Tomography

  benefit of sparse regularization!

- Robust "Compressiveness" is allowed but ...
  - NFFT mandatory!
  - careful noise estimation is needed (not explained here)
  - non-linearities remain (handled as noise up to now)

Summary and further work (2/2)

- Other applications?
  - Phase-contrast X-ray imaging (~~deflection~~ → phase change)

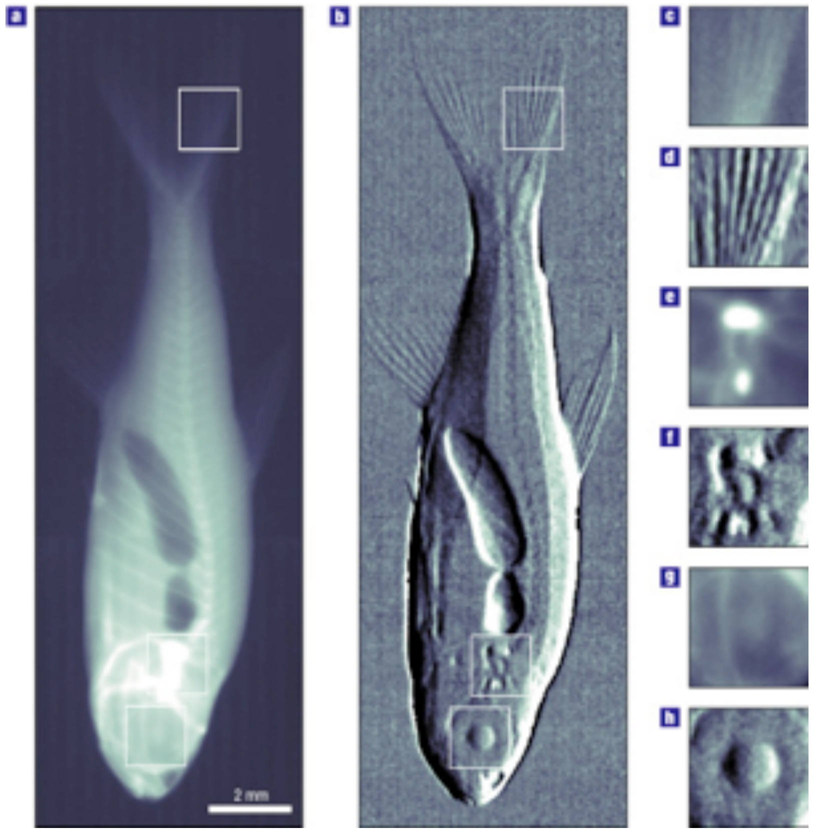

[T. Pfeiffer et al. Nature Physics, 2006]

Summary and further work (2/2)

- Other applications?
  - Phase-contrast X-ray imaging (~~deflection~~ → phase change)
  - Gravitational weak lensing?

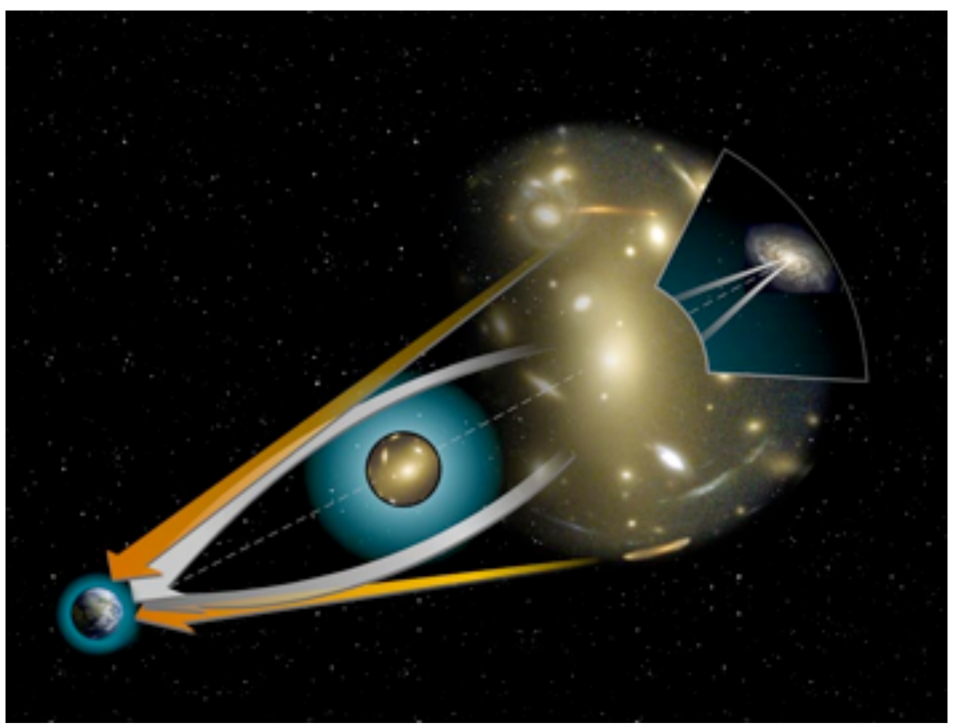

[A. Amara, A. Réfrégier, "Optimal surveys for weak-lensing tomography", MNRAS, 381(3), 1018-1026.]

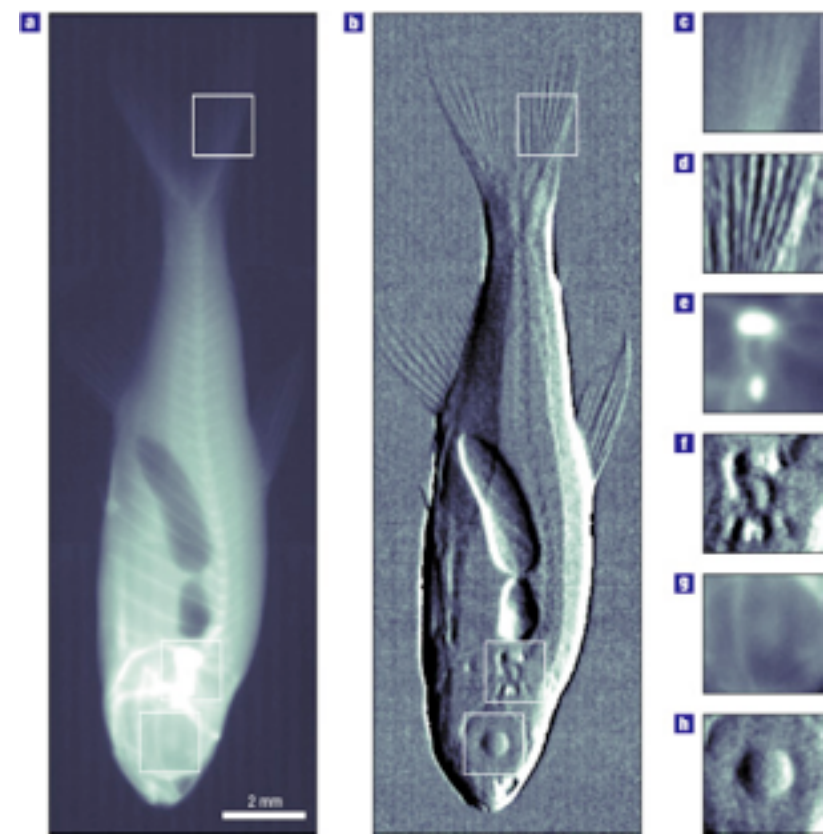

[T. Pfeiffer et al. Nature Physics, 2006]

Thank you!

Further readings

- Prasad Sudhakar, Laurent Jacques, Xavier Dubois, Philippe Antoine, Luc Joannes, "Compressive Imaging and Characterization of Sparse Light Deflection Maps" Submitted, arXiv:1406.6425
- A. Gonzalez, L. Jacques, C. De Vleeschouwer, P. Antoine, "*Compressive Optical Deflectometric Tomography: A Constrained Total-Variation Minimization Approach*", Journal of Inverse Problems and Imaging, vol. 8, no.2, p. 421-457 (2014), arXiv:1209.0654

- G. S. Settles, "Schlieren and Shadowgraph Techniques: Visualizing Phenomena in Transparent Media," Springer, New York, NY, USA, 2001.
- L. Joannes et al., "Phase-shifting schlieren: high-resolution quantitative schlieren that uses the phase-shifting technique principle," Applied optics, 2003.
- G. Puy, et al., "Universal and efficient compressed sensing by spread spectrum and application to realistic Fourier imaging techniques," Journal on Adv. in Sig. Proc., 2012.
- E. Candès et al., "Sparsity and incoherence in compressive sampling," Inverse problems, 2007.
- A. Chambolle et al., "A first-order primal-dual algorithm for convex problems with applications to imaging," Journal of Mathematical Imaging and Vision, 2011.